DISENTANGLING AND INTEGRATING RELATIONAL AND SENSORY INFORMATION IN TRANSFORMER ARCHITECTURES

Anonymous authors
Paper under double-blind review

ABSTRACT

Relational reasoning is a central component of generally intelligent systems, enabling robust and data-efficient inductive generalization. Recent empirical evidence shows that many existing neural architectures, including Transformers, struggle with tasks requiring relational reasoning. In this work, we distinguish between two types of information: *sensory* information about the properties of individual objects, and *relational* information about the relationships between objects. While neural attention provides a powerful mechanism for controlling the flow of sensory information between objects, the Transformer lacks an explicit computational mechanism for routing and processing relational information. To address this limitation, we propose an architectural extension of the Transformer framework that we call the *Dual Attention Transformer (DAT)*, featuring two distinct attention mechanisms: sensory attention for directing the flow of sensory information, and a novel relational attention mechanism for directing the flow of relational information. We empirically evaluate *DAT* on a diverse set of tasks ranging from synthetic relational benchmarks to complex real-world tasks such as language modeling and visual processing. Our results demonstrate that integrating explicit relational computational mechanisms into the Transformer architecture leads to significant performance gains in terms of data efficiency and parameter efficiency.

1 INTRODUCTION

A central goal of machine learning research is to develop universal architectures capable of learning and reasoning across a wide range of tasks and data modalities. Scientific approaches to understanding human and animal intelligence seek to explain intelligent behavior using a small set of fundamental principles [1]. However, machine intelligence, there exists a tension between the objective of developing a general architecture and the need to incorporate inductive biases that are beneficial for specific tasks [2, 3]. When faced with finite training data and numerous solutions to empirical risk minimization, inductive biases steer the learning algorithm towards solutions with desirable properties, enhancing data efficiency and generalization. A core scientific challenge of machine learning is to identify a complete and broadly applicable set of inductive biases that promote robust, flexible, and data-efficient learning across diverse real-world problems.

The Transformer architecture [4] offers a promising starting point for designing versatile, general-purpose machine learning frameworks. By operating over sets or sequences of objects, Transformers are able to support highly-general input and output modalities. More importantly, neural attention provides an effective computational mechanism for dynamically routing information between different elements in the input, enabling iterative contextual processing. This has led to remarkable empirical success across several domains, including language [5–9] and visual processing [10–12].

However, recent work has shown that Transformers struggle to efficiently learn tasks involving relational reasoning [13–22]. Relational reasoning is a central component of generally intelligent systems, and is believed to underlie human abilities for abstraction and systematic generalization [23–25]. The power of relational reasoning lies in its capacity to generate inferences and generalizations in systematic and novel ways, which can ultimately lead to universal inductive generalization from a finite set of observations to an infinite set of novel instances [26]. The lack of support for efficient and robust relational learning and abstraction remains a major limitation of the Transformer framework.

In this work, drawing an analogy to neural systems in the brain [27], we distinguish between two types of information: *sensory* information which encodes the properties of individual objects, and *relational* information which encodes the relationships between objects. Accordingly, we posit the following explanation for the Transformer's limited abilities in relational learning: while neural attention provides a powerful mechanism for routing *sensory* information in the input, the Transformer lacks an explicit computational mechanism for routing and processing *relational* information between objects in the input. We argue that a unified architecture for general machine intelligence requires computational mechanisms and inductive biases for processing both sensory and relational information. Towards this goal, we propose an extension of the Transformer framework that enables explicit routing and processing of both sensory and relational information.

To introduce our proposed method at a high-level, it is useful to view standard Transformers as an instance of a broader neural message-passing computational paradigm that consists of iterative information retrieval followed by local processing. In the general form of a message-passing procedure, a set of objects $x_1, \ldots, x_n$ are processed via an iterative application of the following steps:

$$\begin{aligned} \text{(Information Retrieval)} \quad & x_i \leftarrow \mathrm{Aggregate}\big(x_i, \{m_{j \to i}\}_{j=1}^n\big), \\ \text{(Local Processing)} \quad & x_i \leftarrow \mathrm{Process}(x_i). \end{aligned} \tag{1}$$

In Transformers, the information retrieval step corresponds to the self-attention mechanism, where the message sent from object j to object i is an encoding of the sender's *sensory* features, $m_{j \to i} = \phi_v(x_j)$. These messages are then aggregated according to some selection criterion based on the receiver's features, determined by softmax attention scores.

To enable explicit relational representation learning, we propose a novel attention mechanism, dubbed *relational attention*, that selectively attends to and routes relational information between objects. In relational attention, the message from the sender object to the receiver object consists of a set of relations between them, which can be expressed as $m_{j \to i} = r(x_i, x_j)$. Here, the relation $r(\cdot, \cdot)$ models a series of comparisons between the pair of objects across different feature dimensions using inner products of feature maps. We integrate this with the standard attention mechanism of Transformers, yielding a variant of multi-head attention for processing both sensory and relational information in parallel. This *Dual Attention* architecture disentangles these two types of information during the aggregation phase and integrates them in the information processing stage.

The contributions of this paper are summarized as follows:

- ***A neural mechanism for routing and processing relational information.*** We introduce a new *relational attention* mechanism that disentangles relational information from sensory information. While standard self-attention models the retrieval of sensory information, relational attention models the retrieval of relational information.
- ***An architectural extension of the Transformer for joint sensory-relational processing.*** We introduce an extension of the Transformer architecture that integrates sensory and relational information through *Dual Attention*—a form of multi-head attention with two distinct types of attention heads. Standard self-attention heads encode sensory information, while relational attention heads encode relational information.
- ***Empirically evaluating the promise of relational computational mechanisms.*** While relational reasoning is believed to be an essential component of general intelligence, the success of relational inductive biases in machine learning has so far been mainly limited to synthetic tasks, despite recent advances in relational architectures [15–22]. We evaluate the *Dual Attention Transformer* architecture on a diverse set of tasks ranging from synthetic relational benchmarks to complex real-world tasks such as language modeling and visual processing. Our results demonstrate that incorporating explicit relational computational mechanisms into the Transformer architecture leads to significant performance gains in terms of data efficiency and parameter efficiency.

2 Disentangling Attention over Sensory and Relational Information

2.1 Standard Attention: Attention over Sensory Information

The attention mechanism of standard Transformers can be understood as a form of neural message-passing that performs selective information retrieval over the sensory information in the context.

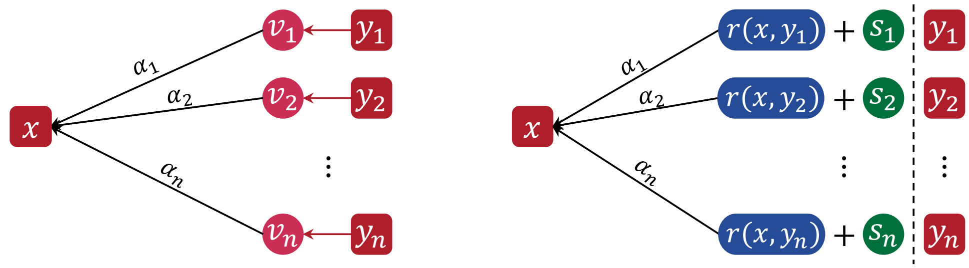

(a) Attention$(x, (y_1, \ldots, y_n))$ (b) RelationalAttention$(x, (y_1, \ldots, y_n))$

Figure 1: Standard self-attention retrieves sensory information v_i about the attributes of individual objects while relational attention retrieves relational information $r(x, y_i)$ about the relationship between the objects in the context and the receiver. Each relation is tagged with a symbol s_i which acts as an abstract variable identifying the sender. In both cases, information is aggregated according to the attention scores α_i, which are computed by a softmax over inner products of queries and keys.

An object emits a query that is compared against the keys of each object in its context via an inner product. A match occurs when the inner product is large, causing an encoding of the features of the attended object to be retrieved and added to the residual stream of the receiver. Formally, attention between an object $x \in \mathbb{R}^d$ and a context $\boldsymbol{y} = (y_1, \ldots, y_n) \in \mathbb{R}^{n \times d}$ takes the form

$$\begin{aligned}\mathrm{Attention}(x, (y_1, \ldots, y_n)) &= \sum_{i=1}^{n} \alpha_i(x, \boldsymbol{y}) \phi_v(y_i), \text{ where,} \\ \alpha(x, \boldsymbol{y}) &= \mathrm{Softmax}\big(\big[\big\langle \phi_q^{\mathrm{attn}}(x), \phi_k^{\mathrm{attn}}(y_i) \big\rangle\big]_{i=1}^{n} \big),\end{aligned} \tag{2}$$

where $\phi_q^{\mathrm{attn}}, \phi_k^{\mathrm{attn}}$ are learnable query and key maps controlling the selection criterion, and ϕ_v is a learnable value map controlling what information about y_i is sent. The attention scores $\alpha(x, \boldsymbol{y})$ are used to retrieve a convex combination of the values, where $\alpha_i(x, \boldsymbol{y})$ denotes the i-th component.

Here, the retrieved information is *sensory*, comprising the features and attributes of individual objects in the context. For this reason, we refer to standard neural attention as "sensory attention".

2.2 Relational Attention: Attention over Relational Information

Standard neural attention does not explicitly capture information about the *relationship* between the sender and the receiver, making relational learning in standard Transformers inefficient [13–22]. We propose *relational attention*, a novel attention mechanism for dynamically routing relational information between objects. Under the message-passing view of eq. (1), relational attention represents an operation where the message from one object to another encodes the relationship between them.

Mirroring standard attention, this operation begins with each object emitting a query and a key, which are compared via an inner product to compute attention scores determining which objects to attend to. Next, instead of retrieving the sensory features of the selected object, relational attention retrieves the *relation* between the two objects—defined as a series of comparisons between the two objects under different feature subspaces. In addition, a symbolic identifier is sent to indicate the identity of the sender to the receiver. Mathematically, this operation is defined as follows.

$$\begin{aligned}\mathrm{RelationalAttention}(x, (y_1, \ldots, y_n)) &= \sum_{i=1}^{n} \alpha_i(x, \boldsymbol{y}) \big(r(x, y_i) W_r + s_i W_s \big), \text{ where,} \\ \alpha(x, \boldsymbol{y}) &= \mathrm{Softmax}\big(\big[\big\langle \phi_q^{\mathrm{attn}}(x), \phi_k^{\mathrm{attn}}(y_i) \big\rangle\big]_{i=1}^{n} \big), \\ r(x, y_i) &= \big(\big\langle \phi_{q,\ell}^{\mathrm{rel}}(x), \phi_{k,\ell}^{\mathrm{rel}}(y_i) \big\rangle \big)_{\ell \in [d_r]}, \\ (s_1, \ldots, s_n) &= \mathrm{SymbolRetriever}(\boldsymbol{y};\, S_{\mathrm{lib}})\end{aligned} \tag{3}$$

Thus, relational attention between the object x and the context $\boldsymbol{y} = (y_1, \ldots, y_n)$ retrieves a convex combination of the relation vectors $\{r(x, y_i)\}_{i=1}^{n}$, representing x's relationship with each object in the context. Relational attention also retrieves a symbol vector s_i, selected from a learned symbol library S_{lib}, that encodes the identity information of the attended object. The role and implementation of the symbols will be discussed in the next subsection. As with standard attention, $\phi_q^{\text{attn}}, \phi_k^{\text{attn}}$ are learned feature maps that govern which object(s) in the context to attend to. Another set of query and key feature maps, $\phi_{q,\ell}^{\text{rel}}, \phi_{k,\ell}^{\text{rel}}, \ell \in [d_r]$, are learned to represent the relation between the sender and the receiver. For each $\ell \in [d_r]$, the feature maps $\phi_{q,\ell}^{\text{rel}}, \phi_{k,\ell}^{\text{rel}}$ extract specific attributes from the object pair, which are compared by an inner product. This produces a d_r-dimensional relation vector representing a fine-grained series of comparisons $(\langle \phi_{q,\ell}^{\text{rel}}(x), \phi_{k,\ell}^{\text{rel}}(y_i) \rangle)_{\ell \in [d_r]}$ across different feature subspaces.

In certain tasks [20–22], a useful inductive bias on the relations function $r(\cdot, \cdot)$ is symmetry; i.e., $r(x, y) = r(y, x)$, $\forall x, y$. This corresponds to using the same feature filter for the query and key maps, $\phi_q^{\text{rel}} = \phi_k^{\text{rel}}$. This adds structure to the relation function, transforming it into a positive semi-definite kernel that defines a pseudometric on the object space, along with a corresponding geometry.

2.3 Symbol Assignment Mechanisms

To process relational information effectively, the receiver must have two pieces of information: 1) its relationship to the objects in its context, and 2) the identity of the object associated with each relation. In relational attention, the former is captured by $r(x, y_i)$ and the latter by s_i. The symbols s_i are used to tag each relation with the identity information of the sender.

The symbol s_i identifies or points to the object y_i, but, importantly, is designed to not fully encode the features of the object. Instead, the symbols s_i function as abstract references to objects, perhaps viewed as a connectionist analog of pointers in traditional symbolic systems. In particular, by drawing symbol vectors from a finite library S_{lib} to identify objects, relational attention maintains a relation-centric representation. This separation between sensory and relational information is key to making relational attention disentangled from sensory features, enabling generalization across relations.

The notion of the “identity” of an object can vary depending on context. In this work, we consider modeling three types of identifiers: 1) position, 2) relative position, or 3) an equivalence class over features. For each type of identifier, we model a corresponding symbol assignment mechanism [21]. We find that different symbol assignment mechanisms are more effective in different domains.

Positional Symbols. In some applications, it is sufficient to identify objects through their position in the input sequence. We maintain a library of symbols $S_{\text{lib}} = (s_1, \ldots, s_{\texttt{max\_len}}) \in \mathbb{R}^{\texttt{max\_len} \times d}$ and assign s_i to the i-th object in the sequence. These are essentially learned positional embeddings.

Position-Relative Symbols. Often, the *relative* position with respect to the receiver is a more useful identifier than absolute position. This can be implemented with position-relative embeddings. We learn a symbol library $S_{\text{lib}} = (s_{-\Delta}, \ldots, s_{-1}, s_0, s_1, \ldots, s_\Delta) \in \mathbb{R}^{(2\Delta+1) \times d}$, where Δ is the maximum relative position, and relational attention becomes $\sum_j \alpha_{ij} (r(x_i, x_j)\, W_r + s_{j-i}\, W_s)$.

Symbolic Attention. In certain domains, some information about the objects' features is necessary to identify them for the purposes of relational processing. Yet, to maintain a relational inductive bias, we would like to avoid sending a full encoding of object-level features. In symbolic attention, we learn a set of symbol vectors, $S_{\text{lib}} = (s_1, \ldots, s_{n_s}) \in \mathbb{R}^{n_s \times d}$ and a matching set of feature templates $F_{\text{lib}} = (f_1, \ldots, f_{n_s})$. We retrieve a symbol for each object by an attention operation that matches the input vectors x_i against the feature templates f_j and retrieves symbols s_j.

$$\mathrm{SymbolicAttention}(\boldsymbol{x}) = \mathrm{Softmax}\big((\boldsymbol{x}\, W_q)\, F_{\text{lib}}^\top\big) S_{\text{lib}}. \tag{4}$$

Here, $S_{\text{lib}}, F_{\text{lib}}, W_q$ are learned parameters. This can be thought of as implementing a learned differentiable “equivalence class map” over feature embeddings. Crucially, the number of symbols (i.e., feature equivalence classes) is *finite*, which enables relational attention to still produce a relation-centric representation while tagging the relations with the necessary identifier.

2.4 What Class of Functions can Relational Attention Compute?

To give some intuition about the type of computation that relational attention can perform, we present the following approximation result. The following theorem states that relational attention can approximate any function on $\mathcal{X} \times \mathcal{Y}^n$ that 1) selects an element in $(y_1, \ldots, y_n)$, then 2) computes a relation with it. Both the selection criterion and the relation function are arbitrary, and the selection criterion can be query-dependent. The formal statement and proof are given in Appendix A.

Theorem 1 (Informal)**.** *Let* $\mathrm{Select} : \mathcal{X} \times \mathcal{Y}^n \to \mathcal{Y}$ *be an arbitrary preference selection function, which selects an element among* $(y_1, \ldots, y_n)$ *based on a query-dependent preorder relation* $\{\preccurlyeq_x\}_{x \in \mathcal{X}}$. *Let*

$\mathrm{Rel} : \mathcal{X} \times \mathcal{Y} \to \mathbb{R}^{d_r}$ *be an arbitrary continuous relation function on* $\mathcal{X} \times \mathcal{Y}$*. There exists a relational attention module that approximates the function* $\mathrm{Rel}(x, \mathrm{Select}(x, \boldsymbol{y}))$ *to arbitrary precision.*

3 Integrating Attention over Sensory and Relational Information

3.1 Dual Attention

One of the keys to the success of the Transformer architecture is the use of so-called *multi-head* attention. This involves computing multiple attention operations in parallel at each layer and concatenating the output, enabling the model to learn multiple useful criteria for routing information between objects. However, in standard Transformers, these attention heads focus solely on routing sensory information, lacking explicit support for routing *relational* information between objects.

We posit that both sensory and relational information are crucial for robust and flexible learning over sequences or collections of objects. To this end, we propose an extension of multi-head attention comprising two distinct types of attention heads: sensory attention (i.e., standard self-attention), and relational attention. This yields a powerful mechanism for dynamically routing both sensory and relational information in parallel. Our hypothesis is that by having access to both computational mechanism, the model can learn to select between them based on the current task or context, as well as compose them to create highly-expressive and flexible computational circuits.

Algorithm 1 describes the proposed module, referred to as *dual attention*. The number of sensory-attention heads n_h^{sa} and number of relational attention heads n_h^{ra} are hyperparameters. The sensory-attention heads attend to sensory information while the relational attention heads attend to relational information. The combined $n_h := n_h^{sa} + n_h^{ra}$ heads are then concatenated to produce the output. The result is a representation of contextual information with integrated sensory and relational components. Appendix B provides further discussion on the details of the architecture and its implementation.

Algorithm 1: Dual Attention

Input: $\boldsymbol{x} = (x_1, \ldots, x_n) \in \mathbb{R}^{n \times d}$

`Compute self-attention heads`

$$\boldsymbol{\alpha}^{(h)} \leftarrow \mathrm{Softmax}\big((\boldsymbol{x}\, W_{q,h}^{\mathrm{attn}})(\boldsymbol{x}\, W_{k,h}^{\mathrm{attn}})^\intercal\big), \qquad h \in [n_h^{sa}]$$

$$e_i^{(h)} \leftarrow \sum_j \alpha_{ij}^{(h)} x_j\, W_v^h, \qquad i \in [n], h \in [n_h^{sa}]$$

$$e_i \leftarrow \mathrm{concat}\big(e_i^{(1)}, \ldots, e_i^{(n_h^{sa})}\big)\, W_o^{sa}, \qquad i \in [n]$$

`Assign symbols:` $\boldsymbol{s} = (s_1, \ldots, s_n) \leftarrow \mathrm{SymbolRetriever}(\boldsymbol{x};\, S_{\mathrm{lib}})$

`Compute relational attention heads`

$$\boldsymbol{\alpha}^{(h)} \leftarrow \mathrm{Softmax}\big((\boldsymbol{x}\, W_{q,h}^{\mathrm{attn}})(\boldsymbol{x}\, W_{k,h}^{\mathrm{attn}})^\intercal\big), \qquad h \in [n_h^{ra}]$$

$$\boldsymbol{r}_{ij} \leftarrow \big(\langle x_i\, W_{q,\ell}^{\mathrm{rel}}, x_j\, W_{k,\ell}^{\mathrm{rel}}\rangle\big)_{\ell \in [d_r]} \qquad i, j \in [n]$$

$$a_i^{(h)} \leftarrow \sum_j \alpha_{ij}^{(h)} \big(\boldsymbol{r}_{ij}\, W_r^h + s_j\, W_s^h\big), \qquad i \in [n],\ h \in [n_h^{ra}]$$

$$a_i \leftarrow \mathrm{concat}\big(a_i^{(1)}, \ldots, a_i^{(n_h^{ra})}\big) W_o^{ra}, \qquad i \in [n]$$

Output: $\big(\mathrm{concat}(e_i, a_i)\big)_{i=1}^n$

Attention Masks & Causality. Any type of attention mask (e.g., causal mask for autoregressive language modeling) can be implemented in relational attention in the same way as for standard self-attention (i.e., mask is added to α_{ij}^h pre-softmax).

Positional Encoding. There exists different methods in the literature for encoding positional information in the Transformer architecture. For example, [4] propose adding positional embeddings to the input, [28] propose adding relative-positional embeddings at each attention operation, and [29] propose rotary positional embeddings (RoPE) which apply a position-dependent map to the queries and keys pre-softmax. These methods are compatible with dual attention and are configurable options in our public implementation.

Computational complexity. The computational complexity of relational attention scales similarly to standard self-attention with a $O(n^2)$ dependence on sequence length. Like standard attention, relational attention can be computed in parallel via efficient matrix multiplication operations.

Symmetric relations. A symmetry constraint can be injected into the relations $\boldsymbol{r}_{ij}$ by imposing that $W_q^{\mathrm{rel}} = W_k^{\mathrm{rel}}$, which is a useful inductive bias when the task-relevant relations have this structure.

3.2 The Dual Attention Transformer Architecture

The standard Transformer architecture is composed of repeated blocks of attention (information retrieval) followed by an MLP (local processing). Our proposed *Dual Attention Transformer* follows this same structure, but replaces multi-head self-attention with dual attention. At each layer, dual attention dynamically retrieves both sensory and relational information from the previous level of computation, which is then processed locally by an MLP. Algorithms 2 and 3 defines an encoder and decoder block with dual attention. Composing these blocks yields the Dual Attention Transformer architecture.

Algorithm 2: Dual Attention Encoder Block

Input : $\boldsymbol{x} \in \mathbb{R}^{n \times d}$

$\boldsymbol{x} \leftarrow \mathrm{Norm}(\boldsymbol{x} + \mathrm{DualAttn}(\boldsymbol{x}))$
$\boldsymbol{x} \leftarrow \mathrm{Norm}(\boldsymbol{x} + \mathrm{MLP}(\boldsymbol{x}))$

Output: $\boldsymbol{x}$

Algorithm 3: Dual Attention Decoder Block

Input : $\boldsymbol{x}, \boldsymbol{y} \in \mathbb{R}^{n \times d}$

$\boldsymbol{x} \leftarrow \mathrm{Norm}(\boldsymbol{x} + \mathrm{DualAttn}(\boldsymbol{x}))$
$\boldsymbol{x} \leftarrow \mathrm{Norm}(\boldsymbol{x} + \mathrm{CrossAttn}(\boldsymbol{x}, \boldsymbol{y}))$
$\boldsymbol{x} \leftarrow \mathrm{Norm}(\boldsymbol{x} + \mathrm{MLP}(\boldsymbol{x}))$

Output: $\boldsymbol{x}$

The Dual Attention Transformer framework supports all architectural variants of the standard Transformer, making it applicable to a wide range of task paradigms. An encoder-decoder architecture with causal dual-head attention in the decoder can be applied to sequence-to-sequence tasks, as in the original Transformer paper [4]. An encoder-only architecture can be used for a BERT-style language embedding model [6] or a *ViT*-style vision model [10]. A decoder-only architecture with causal dual-head attention can be used for autoregressive language modeling.

4 Empirical Evaluation

We empirically evaluate the Dual Attention Transformer (abbreviated, *DAT*) architecture on a range of tasks spanning different domains and modalities. Our goal is to assess the impact of integrating relational inductive biases into the Transformer architecture. We begin with a synthetic relational learning benchmark to evaluate *DAT*'s relational computational mechanisms in a more controlled setting. We then proceed to evaluate the proposed architecture on more complex real-world tasks, including mathematical problem-solving, image recognition, and language modeling. These experiments cover multiple task paradigms and architectural variants, including: discriminative (encoder-only architecture), sequence-to-sequence (encoder-decoder), autoregressive language modeling (decoder-only), and vision (*ViT*-style architecture) tasks. For each experiment, we compare a *DAT* model that incorporates both sensory and relational heads against a standard Transformer where all heads are ordinary sensory attention heads. The difference in performance highlights the impact of integrating both types of attention heads, enabling a richer representation of sensory and relational information. We summarize the experimental results below and defer certain experimental details to Appendix C.

4.1 Sample-Efficient Relational Reasoning: Relational Games

We begin our empirical evaluation with the "Relational Games" benchmark for visual relational reasoning contributed by Shanahan et al. [17]. The dataset consists of a family of binary classification tasks, each testing a model's ability to identify a particular visual relationship among a series of objects (see Figure 6 for examples). The input is an RGB image depicting a grid of objects, and the target is a binary classification indicating whether the particular relationship holds for this input. This forms a controlled synthetic setting for evaluating *DAT*'s effectiveness in relational learning.

Our goal in this section is to explore how the relational computational mechanisms of *DAT* affect data-efficiency in relational learning—that is, how much data is necessary to learn a given task. We evaluate *learning curves* by varying the size of the training set, training each model until convergence, and evaluating on a hold-out validation set. We test two configurations of *DAT*: one with only relational attention heads, and one with a combination both sensory and relational heads. We include several Transformer baselines, varying the number of attention heads and the model dimension, controlling for parameter count. The results are depicted in Figure 2.

We find that *DAT* is significantly more sample-efficient, particularly at more difficult tasks. Both configurations of *DAT* are consistently more sample-efficient compared to the standard Transformer. The effect is particularly dramatic on the '`match pattern`' task which is the most difficult and requires identifying a second-order relation (i.e., a relation between relations). We note that these tasks are purely relational in the sense that pairwise same/different relations between objects are a sufficient statistic for predicting the target. This suggests that relational attention is sufficient for solving the task. Indeed, the *DAT* variant with only relational heads performs marginally better than the variant with a combination of both sensory and relational heads. Notably, however, the difference is only marginal, suggesting that the model is able to learn to select the computational mechanisms that are most relevant to the given task. We provide further discussion in Appendix C.1, including results comparing against previously-proposed relational architectures with stricter inductive biases.

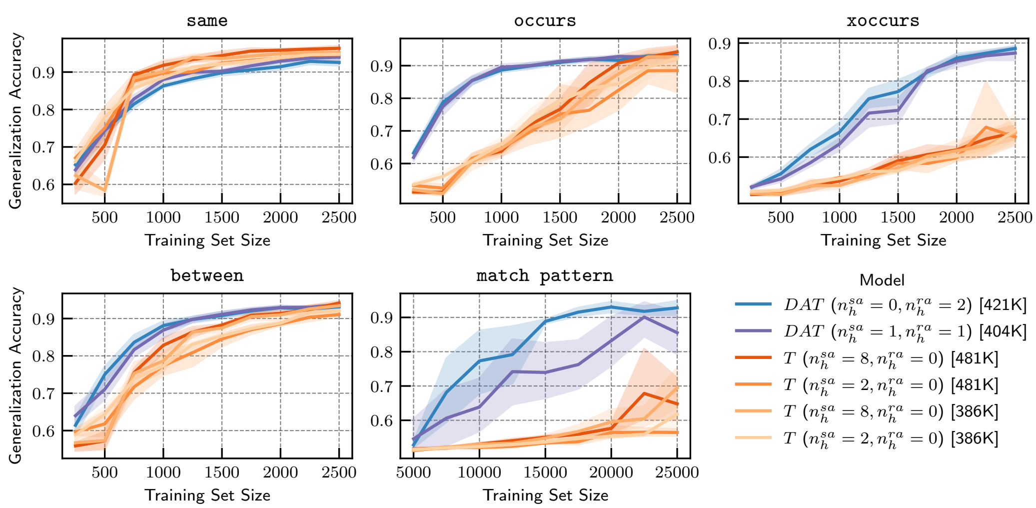

Figure 2: Learning curves on the relational games benchmark. Each subplot corresponds to a different task. Numbers in square brackets in legend labels indicate parameter counts. Solid lines indicate the mean over 5 trials with different random seeds and the shaded regions indicate bootstrap 95% confidence intervals. *DAT* is more data-efficient at relational learning compared to a Transformer.

4.2 Relational Inductive Biases for Symbolic Reasoning in Sequence-to-Sequence tasks: Mathematical Problem Solving

Next, we evaluate *DAT* on a set of mathematical problem-solving tasks based on the benchmark contributed by Saxton et al. [30]. Mathematical problem-solving is an interesting test for neural models because it requires more than statistical pattern recognition—it requires inferring laws, axioms, and symbol manipulation rules. The benchmark consists of a suite of mathematical problem-solving tasks, with each task's dataset consisting of a set of question-answer pairs. The tasks range across several topics including solving equations, adding polynomials, expanding polynomials, differentiating functions, predicting the next term in a sequence, etc. An example of a question in the "`polynomials__expand`" task is "Expand $(5x-3)(2x+1)$" with the target answer "$10x^2-x-3$". This is modeled as a sequence-to-sequence task with character-level encoding.

We compare *DAT* against Transformers using an encoder-decoder architecture. The encoder processes the question, and the decoder autoregressively generates the answer while cross-attending to the encoder. We explore how performance scales with model size by varying the number of layers. In the Transformer, all attention heads are standard self-attention with $n_h^{sa}=8$, while in *DAT* we have a combination of both types of attention heads with $n_h^{sa}=n_h^{ra}=4$. The *DAT* models use position-relative symbols as their symbol assignment mechanism.

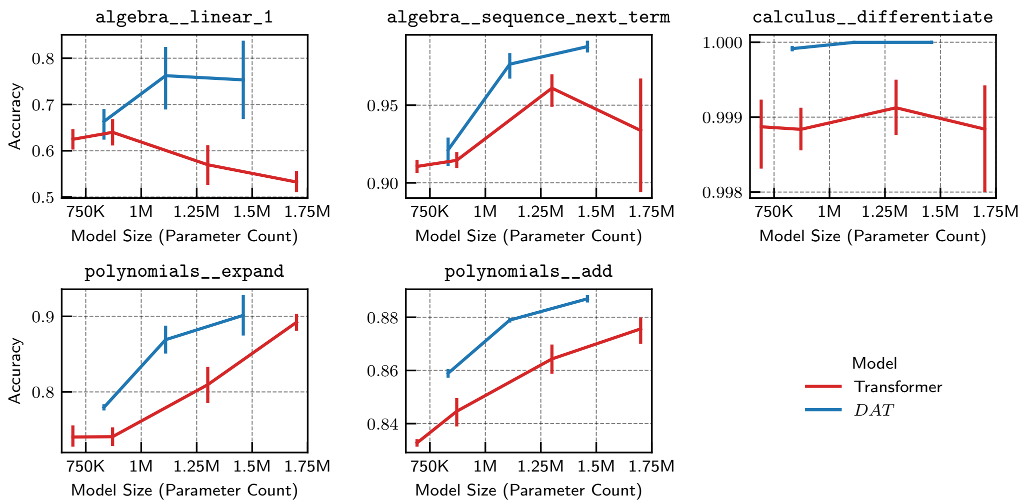

Figure 3: Average character-level accuracy on different mathematical problem-solving tasks measured at different model sizes. Error bars indicate bootstrap 95% confidence intervals over 5 trials. *DAT* outperforms a standard Transformer across model sizes, suggesting that relational computational mechanisms confer benefits on sequence-to-sequence tasks that involve symbolic computation.

Dataset	Model	Parameter Count	# Layers	d_{model}	n_h^{sa}	n_h^{ra}	Accuracy
CIFAR-10	*ViT*	7.1M	8	384	12	0	$86.4 \pm 0.1\%$
	ViDAT	6.0M	8	384	6	6	$\mathbf{89.7 \pm 0.1\%}$
CIFAR-100	*ViT*	7.2M	8	384	12	0	$68.8 \pm 0.2\%$
	ViDAT	6.1M	8	384	6	6	$\mathbf{70.5 \pm 0.1\%}$

Table 1: Classification accuracy on image recognition with the CIFAR-10 and CIFAR-100 datasets. Each training configuration is repeated 10 times with different random seeds; we report the mean accuracy $\pm$ the standard error of mean. *DAT* outperforms a standard Vision Transformer, suggesting that relational computational mechanisms are useful for visual processing tasks.

Figure 3 depicts the character-level accuracy for *DAT* and Transformers across varying model sizes. We find that the *DAT* model outperforms the standard Transformer at all model scales and across all tested tasks. This suggests that the relational computational mechanisms of *DAT* are beneficial for the type of symbolic processing involved in solving mathematical problems.

4.3 Visual Processing with Relational Inductive Biases

As a general sequence model, the Transformer architecture can be applied to visual inputs by dividing an image into patches that are then flattened, linearly embedded into vectors, and passed in as a sequence. Through a series of attention and MLP operations, the visual input is processed for the downstream visual task. This architecture is referred to as a Vision Transformer (*ViT*) [10]. Although Transformers lack the explicit spatial inductive biases found in models like convolutional networks, recent work has demonstrated its effectiveness at scale [12], suggesting that attention is a versatile computational mechanism applicable across several data modalities.

In this section, we explore how the relational computational mechanisms introduced in *DAT*—namely, relational attention—impact visual processing tasks. We hypothesize that visual processing benefits from attending to both sensory and relational information. That is, when processing a local region of a visual input (e.g., a patch, object, or object part), it is useful consider not only the sensory features of other regions but also the relationships between these regions. For example, this captures information about similar objects occurring in multiple places in the scene, or objects which are similar across some attributes (e.g., texture) but different across others (e.g., color).

We evaluate a *ViT*-style *DAT* architecture (*ViDAT*), and compare it against a standard *ViT* on the CIFAR image recognition benchmarks [31]. We train directly on CIFAR-10 and CIFAR-100,

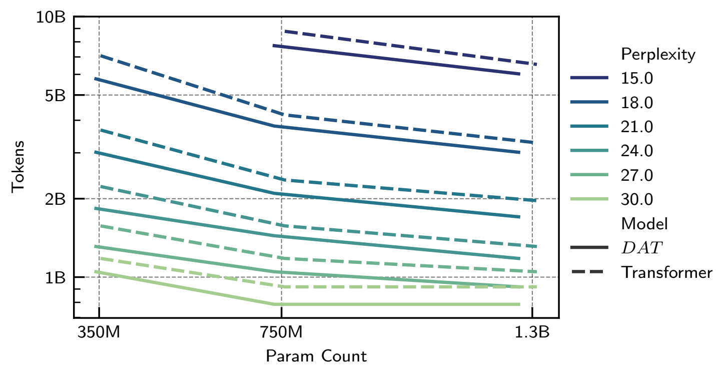

Figure 4: A representation of the amount of data (in tokens) needed to reach a given level of language modeling performance (in perplexity) at each model size. The *DAT* architecture demonstrates greater data and parameter efficiency compared to standard Transformers.

respectively, without pretraining on larger datasets. During training, we use random cropping, MixUp [32], and CutMix [33] as data augmentation techniques. We evaluate 8-layer models with $d_{\text{model}} = d_{\text{ff}} = 384$. The *ViT* model has $n_h^{sa} = 12$ standard self-attention heads, while the *DAT* model uses both sensory and relational heads, with an even split of $n_h^{sa} = n_h^{ra} = 6$. We use symmetric relations $\boldsymbol{r}_{ij}$ based on the intuition that visual processing involves symmetric attribute-similarity relations. We use position-relative symbols as the symbol assignment mechanism. In Appendix C.3, we present ablations, additional results, and provide further discussion.

Table 1 reports the classification accuracy of each model. We find that the *ViDAT* architecture outperforms the standard *ViT* architecture across both datasets, suggesting that the relational computational mechanisms confer benefits in visual processing. These experiments show that relational inductive biases can be useful for image recognition. We hypothesize that relational processing is even more important in visual tasks requiring complex scene parsing, where reasoning about the relationships between constituent objects is essential. Recent work on scene understanding in large vision-language models supports this view [34–36]. We leave exploration of these more complex tasks to future work.

4.4 Relational Inductive Biases in Language Modeling

Language understanding involves processing and organizing relational information, such as syntactic structures, semantic roles, and contextual dependencies, to extract meaning from words and their connections within sentences. Transformers have been remarkably effective at language modeling, with neural scaling laws demonstrating that increasing model size and dataset size result in predictable improvements in performance across a range of language tasks [8]. While the standard attention mechanism of Transformers is able to capture simple positional and syntactic relations in its attention scores, this is only used to control the flow of information between tokens rather than explicitly encoding relational information in the latent embeddings themselves. The relational attention mechanism of *DAT* enables explicitly learning relational contextual information that is directly encoded in each token's latent embedding.

In this section, we evaluate *DAT* on causal language modeling, exploring the impact of its relational computational mechanisms in the domain of language. We use a decoder-only architecture, where the model receives a sequence of tokens as input and is trained to causally predict the next token at each position. We train on 10 billion GPT2 tokens of the FineWeb-Edu dataset [37], which is a curated dataset of high-quality educational text data from CommonCrawl. We train models at multiple parameter scales to study the scaling properties of *DAT* on language modeling with respect to both model size and data size. Details of training and architectural hyperparameters are given in Appendix C.4, together with further discussion of the results.

Figure 4 depicts the scaling properties of *DAT*'s language modeling performance with respect to model size and data size, compared to a standard Transformer. We observe that *DAT* demonstrates greater data and parameter efficiency, achieving improved performance across model and data scales. This suggests that *DAT*'s relational computational mechanisms confers benefits in language processing.

Beyond performance improvements in language modeling as measured by a drop in perplexity, we also find evidence that relational attention encodes human-interpretable semantic relations. Figure 5 depicts a visualization of the relations $\boldsymbol{r}_{ij}$ learned by a *DAT* language model. We observe that

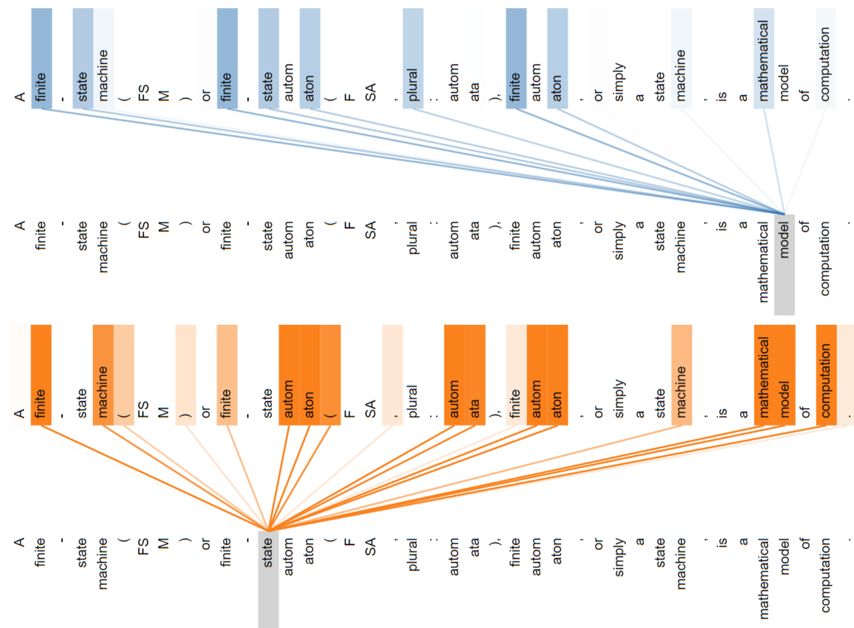

Figure 5: Relational attention in *DAT* language models encodes human-interpretable semantic relations. A visualization of the relations $\boldsymbol{r}_{ij}$ learned by a 24-layer 343M-parameter *DAT* language model. **Top.** Visualization of one relation dimension in the first layer, focusing on the token `'model'`, which has high activation with the tokens `'state'`, `'machine'`, and `'mathematical'`. **Bottom.** Visualization of one relation dimension in the twelfth layer, focusing on the token `'state'`, which has high activation with the tokens `'mathematical'`, `'model'`, and `'computation'`.

the relations learned by relational attention tend to encode semantic relations, rather than syntactic relations. That is, relational activations $\boldsymbol{r}_{ij} \in \mathbb{R}^{d_r}$ are large between tokens with related *meanings*. This is in contrast to the attention scores of standard Transformers, where attention heads typically focus on position, syntax, and punctuation [38–40], rather than semantic content. We believe that further exploration of this phenomenon from a mechanistic interpretability perspective could offer an exciting avenue for future research.

5 Conclusion

Summary. The standard attention mechanism of Transformers provides a versatile mechanism for retrieval of sensory information from a given context, but does not explicitly support retrieval of relational information. In this work, we presented an extension of the Transformer architecture that disentangles and integrates sensory and relational information through a variant of multi-head attention with two distinct types of attention heads: standard self-attention for sensory information and a novel *relational attention* mechanism for relational information. We empirically evaluate this architecture and find that it yields performance improvements across a range of tasks and modalities.

Limitations & Future Work. The proposed architecture introduces several hyperparameters and possible configurations. Although we carried out ablations on the major configuration choices (e.g., composition of head types, symmetry, symbol assignment mechanisms), an expanded empirical investigation would help develop an improved understanding of the behavior of this architecture under different configurations. We also note that our implementation of the Dual-Attention Transformer currently lacks the hardware-aware optimizations available for standard Transformers (e.g., Flash-Attention [41]), which results in slower performance, though we expect similar optimizations to be possible. An important direction for future work is the mechanistic interpretability [40, 42, 43] of *DAT* models, focusing on identifying specific circuits that perform key computations to better understand the performance improvements observed in complex domains like language modeling.

Code and Reproducibility

Our implementation of the Dual Attention Transformer architecture is open-sourced and published as a Python package. Pre-trained model weights, including the 1.3B-parameter *DAT* language model, are made publicly available and can be loaded directly using the package. Additionally, we provide code for running the experiments described in this paper, along with instructions for reproducing our results and access to the experimental logs. Links will be included in the de-anonymized camera-ready version.

References

[1] Gary F Marcus. "The algebraic mind: Integrating connectionism and cognitive science". MIT press, 2003 (cited on page 1).

[2] David H Wolpert, William G Macready, et al. "No free lunch theorems for search". Tech. rep. Citeseer, 1995 (cited on page 1).

[3] Jonathan Baxter. "A model of inductive bias learning". In: *Journal of artificial intelligence research* (2000) (cited on page 1).

[4] Ashish Vaswani et al. "Attention Is All You Need". In: *Advances in neural information processing systems* (2017) (cited on pages 1, 5, 6, 18).

[5] Alec Radford et al. "Improving Language Understanding by Generative Pre-Training". In: (2018) (cited on page 1).

[6] Jacob Devlin et al. "BERT: Pre-training of Deep Bidirectional Transformers for Language Understanding". In: *Proceedings of the 2019 Conference of the North American Chapter of the Association for Computational Linguistics*. Association for Computational Linguistics, June 2019 (cited on pages 1, 6).

[7] Alec Radford et al. "Language models are unsupervised multitask learners". In: *OpenAI blog* (2019) (cited on pages 1, 23).

[8] Jared Kaplan et al. "Scaling Laws for Neural Language Models". 2020. arXiv: 2001.08361 [cs.LG] (cited on pages 1, 9, 23).

[9] Tom B. Brown et al. "Language Models are Few-Shot Learners". 2020. arXiv: 2005.14165 [cs.CL] (cited on page 1).

[10] Alexey Dosovitskiy et al. "An Image is Worth 16x16 Words: Transformers for Image Recognition at Scale". In: *International Conference on Learning Representations*. 2021 (cited on pages 1, 6, 8, 21).

[11] Nicolas Carion et al. "End-to-end object detection with transformers". In: *European conference on computer vision*. Springer. 2020 (cited on page 1).

[12] Xiaohua Zhai et al. "Scaling vision transformers". In: *Proceedings of the IEEE/CVF conference on computer vision and pattern recognition*. 2022 (cited on pages 1, 8).

[13] Brenden Lake and Marco Baroni. "Generalization without systematicity: On the compositional skills of sequence-to-sequence recurrent networks". In: *International conference on machine learning*. PMLR. 2018 (cited on pages 1, 3).

[14] David Barrett et al. "Measuring abstract reasoning in neural networks". In: *International conference on machine learning*. PMLR. 2018 (cited on pages 1, 3).

[15] Adam Santoro et al. "A Simple Neural Network Module for Relational Reasoning". June 2017. arXiv: 1706.01427 [cs] (cited on pages 1–3).

[16] Adam Santoro et al. "Relational Recurrent Neural Networks". In: *Advances in Neural Information Processing Systems*. Curran Associates, Inc., 2018 (cited on pages 1–3).

[17] Murray Shanahan et al. "An Explicitly Relational Neural Network Architecture". In: *Proceedings of the 37th International Conference on Machine Learning*. 2020 (cited on pages 1–3, 6, 19).

[18] Taylor W. Webb, Ishan Sinha, and Jonathan D. Cohen. "Emergent Symbols through Binding in External Memory". Mar. 2021. arXiv: 2012.14601 [cs] (cited on pages 1–3).

[19] Taylor W. Webb et al. "The Relational Bottleneck as an Inductive Bias for Efficient Abstraction". In: *Trends in Cognitive Sciences* (May 2024) (cited on pages 1–3).

[20] Giancarlo Kerg et al. "On Neural Architecture Inductive Biases for Relational Tasks". June 2022. arXiv: 2206.05056 [cs] (cited on pages 1–4, 19).

[21] Awni Altabaa et al. "Abstractors and relational cross-attention: An inductive bias for explicit relational reasoning in Transformers". In: *The Twelfth International Conference on Learning Representations*. 2024 (cited on pages 1–4, 19, 24–26).

[22] Awni Altabaa and John Lafferty. "Learning Hierarchical Relational Representations through Relational Convolutions". Feb. 2024. arXiv: `2310.03240 [cs]` (cited on pages 1–4).

[23] Richard E Snow, Patrick C Kyllonen, Brachia Marshalek, et al. "The topography of ability and learning correlations". In: *Advances in the psychology of human intelligence* (1984) (cited on page 1).

[24] Charles Kemp and Joshua B Tenenbaum. "The discovery of structural form". In: *Proceedings of the National Academy of Sciences* (2008) (cited on page 1).

[25] Keith J Holyoak. "Analogy and relational reasoning". In: *The Oxford handbook of thinking and reasoning* (2012) (cited on page 1).

[26] Anirudh Goyal and Yoshua Bengio. "Inductive biases for deep learning of higher-level cognition". In: *Proceedings of the Royal Society A* (2022) (cited on page 1).

[27] James Newman, Bernard J Baars, and Sung-Bae Cho. "A neural global workspace model for conscious attention". In: *Neural Networks* (1997) (cited on page 2).

[28] Peter Shaw, Jakob Uszkoreit, and Ashish Vaswani. "Self-Attention with Relative Position Representations". In: *Proceedings of the 2018 Conference of the North American Chapter of the Association for Computational Linguistics: Human Language Technologies, Volume 2 (Short Papers)*. Ed. by Marilyn Walker, Heng Ji, and Amanda Stent. New Orleans, Louisiana: Association for Computational Linguistics, June 2018 (cited on page 5).

[29] Jianlin Su et al. "RoFormer: Enhanced Transformer with Rotary Position Embedding". Nov. 2023. arXiv: `2104.09864 [cs]` (cited on pages 5, 18).

[30] David Saxton et al. "Analysing Mathematical Reasoning Abilities of Neural Models". In: *International Conference on Learning Representations*. 2019 (cited on pages 7, 19).

[31] Alex Krizhevsky. "Learning multiple layers of features from tiny images". Tech. rep. 2009 (cited on pages 8, 21).

[32] Hongyi Zhang et al. "mixup: Beyond Empirical Risk Minimization". In: *International Conference on Learning Representations*. 2018 (cited on pages 9, 22).

[33] Sangdoo Yun et al. "Cutmix: Regularization strategy to train strong classifiers with localizable features". In: *Proceedings of the IEEE/CVF international conference on computer vision*. 2019 (cited on pages 9, 22).

[34] Justin Johnson et al. "CLEVR: A Diagnostic Dataset for Compositional Language and Elementary Visual Reasoning". In: *Proceedings of the IEEE Conference on Computer Vision and Pattern Recognition (CVPR)*. 2017 (cited on page 9).

[35] Aimen Zerroug et al. "A benchmark for compositional visual reasoning". In: *Advances in neural information processing systems* (2022) (cited on page 9).

[36] Bingchen Zhao et al. "Benchmarking Multi-Image Understanding in Vision and Language Models: Perception, Knowledge, Reasoning, and Multi-Hop Reasoning". In: *arXiv preprint arXiv:2406.12742* (2024) (cited on page 9).

[37] Anton Lozhkov et al. "FineWeb-Edu". May 2024 (cited on pages 9, 22).

[38] Kevin Clark et al. "What Does BERT Look At? An Analysis of BERT's Attention". 2019. arXiv: `1906.04341 [cs.CL]` (cited on page 10).

[39] Phu Mon Htut et al. "Do Attention Heads in BERT Track Syntactic Dependencies?" 2019. arXiv: `1911.12246 [cs.CL]` (cited on page 10).

[40] Nelson Elhage et al. "A Mathematical Framework for Transformer Circuits". In: *Transformer Circuits Thread* (2021). https://transformer-circuits.pub/2021/framework/index.html (cited on page 10).

[41] Tri Dao et al. "Flashattention: Fast and memory-efficient exact attention with IO-awareness". In: *Advances in Neural Information Processing Systems* (2022) (cited on page 10).

[42] Catherine Olsson et al. "In-context Learning and Induction Heads". In: *Transformer Circuits Thread* (2022). https://transformer-circuits.pub/2022/in-context-learning-and-induction-heads/index.html (cited on page 10).

[43] Kevin Ro Wang et al. "Interpretability in the Wild: a Circuit for Indirect Object Identification in GPT-2 Small". In: *The Eleventh International Conference on Learning Representations*. 2023 (cited on page 10).

[44] Gerard Debreu et al. "Representation of a preference ordering by a numerical function". In: *Decision processes* (1954) (cited on page 14).

[45] Awni Altabaa and John Lafferty. "Approximation of Relation Functions and Attention Mechanisms". Feb. 2024. arXiv: 2402.08856 [cs, stat] (cited on page 15).

[46] Noam Shazeer. "GLU Variants Improve Transformer". Feb. 2020. arXiv: 2002.05202 [cs, stat] (cited on page 18).

[47] Yann N Dauphin et al. "Language modeling with gated convolutional networks". In: *International conference on machine learning*. PMLR. 2017 (cited on page 18).

[48] Dan Hendrycks and Kevin Gimpel. "Gaussian Error Linear Units (GELUs)". 2016. arXiv: 1606.08415 [cs.LG] (cited on page 18).

[49] Hugo Touvron et al. "Llama 2: Open Foundation and Fine-Tuned Chat Models". July 2023. arXiv: 2307.09288 [cs] (cited on page 18).

[50] Jimmy Lei Ba, Jamie Ryan Kiros, and Geoffrey E. Hinton. "Layer Normalization". 2016. arXiv: 1607.06450 [stat.ML] (cited on page 18).

[51] Biao Zhang and Rico Sennrich. "Root mean square layer normalization". In: *Advances in Neural Information Processing Systems* (2019) (cited on page 18).

[52] Ruibin Xiong et al. "On layer normalization in the transformer architecture". In: *International Conference on Machine Learning*. PMLR. 2020 (cited on page 18).

[53] Francesco Locatello et al. "Object-Centric Learning with Slot Attention". Oct. 2020. arXiv: 2006.15055 [cs, stat] (cited on page 19).

[54] Joshua Ainslie et al. "GQA: Training Generalized Multi-Query Transformer Models from Multi-Head Checkpoints". In: *Proceedings of the 2023 Conference on Empirical Methods in Natural Language Processing*. Singapore: Association for Computational Linguistics, 2023 (cited on page 21).

[55] Ekin D. Cubuk et al. "AutoAugment: Learning Augmentation Policies from Data". 2019. arXiv: 1805.09501 [cs.CV] (cited on page 22).

[56] Guilherme Penedo et al. "The FineWeb Datasets: Decanting the Web for the Finest Text Data at Scale". 2024. arXiv: 2406.17557 [cs.CL] (cited on page 22).

[57] Ronen Eldan and Yuanzhi Li. "TinyStories: How Small Can Language Models Be and Still Speak Coherent English?" May 2023. arXiv: 2305.07759 [cs] (cited on page 25).

A Function Class of Relational Attention: a universal approximation result

To gain a better understanding of the types of functions that can be computed by relational attention, we presented a simple approximation result (Theorem 1) in Section 2.4. Here, we will provide a formal statement of the result and prove it.

Recall that relational attention is a mapping on $\mathbb{R}^d \times \mathbb{R}^{n \times d} \to \mathbb{R}^{d_{\text{out}}}$, where d is the dimension of the input objects and d_{out} is the output dimension. For convenience, we denote the "query space" by $\mathcal{X}$ and the "key space" by $\mathcal{Y}$, though both are $\mathbb{R}^d$ in this setting. Relational attention takes as input a query $x \in \mathcal{X}$ and a collection of objects $\boldsymbol{y} = (y_1, \ldots, y_n) \in \mathcal{Y}^n$ and computes the following

$$\mathrm{RA}(x, \boldsymbol{y}) = \sum_{i=1}^{n} \alpha_i(x; \boldsymbol{y}) \big(r(x, y_i)\, W_r + s_i\, W_s \big), \tag{5}$$

$$\alpha(x; \boldsymbol{y}) = \mathrm{Softmax}\Big(\big[\langle \phi_q^{\text{attn}}(x), \phi_k^{\text{attn}}(y_i) \rangle \big]_{i=1}^{n} \Big) \in \Delta^n, \tag{6}$$

$$r(x, y_i) = \big(\langle \phi_{q,\ell}^{\text{rel}}(x), \phi_{k,\ell}^{\text{rel}}(y_i) \rangle \big)_{\ell \in [d_r]} \in \mathbb{R}^{d_r}, \tag{7}$$

$$(s_1, \ldots, s_n) = \mathrm{SymbolRetriever}\,(\boldsymbol{y};\, S_{\text{lib}}) \in \mathbb{R}^{n \times d_{\text{out}}}, \tag{8}$$

where $\phi_q^{\text{attn}}, \phi_k^{\text{attn}}, \phi_{q,\ell}^{\text{rel}}, \phi_{k,\ell}^{\text{rel}} : \mathbb{R}^d \to \mathbb{R}^{d_k}$ are the feature maps defining the attention mechanism and the relation, respectively. For this section, these are multi-layer perceptrons. Note that in Algorithm 1 these are linear maps, but they are preceded by multi-layer perceptron in Algorithms 2 and 3, which makes the overall function class the same. Moreover, for this analysis we will take $W_r = I, d_{\text{out}} = d_r$ and $W_s = 0$. We will later discuss how the role of symbols fits within the message of the result.

The following result states that relational attention can approximate any function of the form: 1) select an object in $(y_1, \ldots, y_n)$ by an arbitrary query-dependent selection criterion, and 2) compute an arbitrary relation $r : \mathcal{X} \times \mathcal{Y} \to \mathbb{R}^{d_r}$ with the selected object. This is formalized below.

To formalize (1), we adopt an abstract and very general formulation of a "selection criterion" in terms of a family of preference preorders, $\{\preccurlyeq_x\}_x$: for each possible query x, the preorder $\preccurlyeq_x$ defines a preference over objects in $\mathcal{Y}$ to be selected. Intuitively, "$y_1 \preccurlyeq_x y_2$" means that y_2 is more relevant to the query x than y_1.

More precisely, for each query $x \in \mathcal{X}$, $\preccurlyeq_x$ is a complete (for each $y_1, y_2 \in \mathcal{Y}$, either $y_1 \preccurlyeq y_2$ or $y_2 \preccurlyeq_x y_1$), reflexive ($y \preccurlyeq_x y$ for all $y \in \mathcal{Y}$), and transitive ($y_1 \preccurlyeq_x y_2$ and $y_2 \preccurlyeq_x y_3$ implies $y_1 \preccurlyeq_x y_3$) relation. For each $x \in \mathcal{X}$, $\preccurlyeq_x$ induces a preordered space $(\mathcal{Y}, \preccurlyeq_x)$. This implicitly defines two additional relations: $\prec_x$ and $\sim_x$. We will write $y_1 \prec_x y_2$ if "$y_1 \preccurlyeq_x y_2$ and not $y_2 \preccurlyeq_x y_1$", and $y_1 \sim y_2$ if "$y_1 \preccurlyeq_x y_2$ and $y_2 \preccurlyeq_x y_1$".

For a collection of objects $\boldsymbol{y} = (y_1, \ldots, y_n) \in \mathcal{Y}^n$ and a query $x \in \mathcal{X}$, the preorder $\preccurlyeq_x$ defines a selection function

$$\mathrm{Select}(x, (y_1, \ldots, y_n)) \coloneqq \max\left((y_1, \ldots, y_n), \texttt{key} = \preccurlyeq_x \right). \tag{9}$$

That is, $\mathrm{Select}(x, \boldsymbol{y})$ returns the most relevant element with respect to the query x. In particular, it returns y_i when $y_i \succ_x y_j,\ \forall j \neq i$ (and may return an arbitrary element if no unique maximal element exists in $(y_1, \ldots, y_n)$).

We will assume some regularity conditions on the family of preorders $\{\preccurlyeq_x\}_x$ which essentially stipulate that: 1) nearby elements in $\mathcal{Y}$ have a similar preference with respect to each x, and 2) nearby queries in $\mathcal{X}$ induce similar preference preorders.

Assumption 1 (Selection criterion is query-continuous and key-continuous)**.** *The family of preorder relations $\{\preccurlyeq_x\}_{x \in \mathcal{X}}$ satisfies the following:*

1. ***Key-continuity.*** *For each $x \in \mathcal{X}$, $\preccurlyeq_x$ is continuous. That is, for any sequence $(y_i)_i$ such that $y_i \preccurlyeq_x z$ and $y_i \to y_\infty$, we have $y_\infty \preccurlyeq_x z$. Equivalently, for any $y \in \mathcal{Y}$, $\{z \in \mathcal{Y} : z \preccurlyeq_x y\}$ and $\{z \in \mathcal{Y} : y \preccurlyeq_x z\}$ are closed sets in $\mathcal{Y}$.*

2. ***Query-continuity.*** *Under key-continuity, Debreu et al. [44] shows that for each $x \in \mathcal{X}$, there exists a continuous in utility function $u_x : \mathcal{Y} \to \mathbb{R}$ for $\preccurlyeq_x$ such that $y_1 \preccurlyeq_x y_2 \iff u_x(y_1) \leq u_x(y_2)$. For query-continuity, we make the further assumption that there exists a family of utility functions $\{u_x : \mathcal{Y} \to \mathbb{R}\}_{x \in \mathcal{X}}$ such that $u(x, y) \coloneqq u_x(y)$ is also continuous in its first argument.*

For technical reasons, for Equation (9) to make sense, we must assume that there exists a unique element to be selected. We formulate this in terms of an assumption on the data distribution of the space $\mathcal{X} \times \mathcal{Y}^n$. This is a technical assumption, and different forms of such an assumption would be possible (e.g., instead condition on this event).

Assumption 2 (Selection is unique almost always)**.** *Let $(x, \boldsymbol{y}) \sim \mathbb{P}_{x,\boldsymbol{y}}$. For each $\varepsilon > 0$, there exists $\eta_\varepsilon > 0$ such that $\min_{j \neq i} |u_x(y_i) - u_x(y_j)| > \eta_\varepsilon$ with probability at least $1 - \varepsilon$.*

Theorem (Function class of relational attention)**.** *Let $\mathcal{X}, \mathcal{Y}$ be compact Euclidean spaces. Let $\{\preccurlyeq_x\}_{x \in \mathcal{X}}$ be an arbitrary family of relevance preorders on $\mathcal{Y}$ which are query-continuous and key-continuous (Assumption 1). Let $\mathrm{Select}(x, (y_1, \ldots, y_n)) = \max((y_1, \ldots, y_n), \texttt{key} = \preccurlyeq_x)$ be the selection function associated with $\{\preccurlyeq_x\}_x$. Let $R : \mathcal{X} \times \mathcal{Y} \to \mathbb{R}^{d_r}$ be an arbitrary continuous relation function. Suppose $x, \boldsymbol{y} \sim \mathbb{P}_{x,\boldsymbol{y}}$ and that Assumption 2 holds (i.e., the data distribution is such that there exists a unique most-relevant element w.h.p). For any $\varepsilon > 0$, there exists multi-layer perceptrons $\phi_q^{\mathrm{attn}}, \phi_k^{\mathrm{attn}}, \phi_q^{\mathrm{rel}}, \phi_k^{\mathrm{rel}}$ and a choice of symbols such that,*

$$\left\|\mathrm{RA}(x, (y_1, \ldots, y_n)) - R(x, \mathrm{Select}(x, (y_1, \ldots, y_n)))\right\|_\infty < \varepsilon$$

Proof. Condition on the event $\mathcal{E} := \{(x, \boldsymbol{y}) \in \mathcal{X} \times \mathcal{Y}^n : \ \min_{j \neq i} |u_x(y_i) - u_x(y_j)| > \eta_\varepsilon\}$. Let $i^* = \arg\max((y_1, \ldots, y_n), \texttt{key} = \preccurlyeq_x) = \arg\max(u_x(y_1), \ldots, u_x(y_n))$. By [45, Theorem 5.1], for any $\varepsilon_1 > 0$, there exists MLPs $\phi_q^{\mathrm{attn}}, \phi_k^{\mathrm{attn}}$ such that $\alpha_{i^*}(x, \boldsymbol{y}) > 1 - \varepsilon_1$ for any $(x, \boldsymbol{y}) \in \mathcal{E}$. That is, the attention score is nearly 1 for the $\preccurlyeq_x$-selected element *uniformly* over inputs in $\mathcal{E}$.

Similarly, by [45, Theorem 3.1], for any $\varepsilon_2 > 0$, there exists MLPs $(\phi_{q,\ell}^{\mathrm{rel}}, \phi_{k,\ell}^{\mathrm{rel}})_{\ell \in [d_r]}$ such that $r(x, y) := (\langle \phi_{q,\ell}^{\mathrm{rel}}(x), \phi_{k,\ell}^{\mathrm{rel}}(y) \rangle)_{\ell \in [d_r]}$ approximates the target relation R uniformly within an error of ε_2,

$$\left\|R(x, y) - r(x, y)\right\|_\infty < \varepsilon_2, \quad \text{Lebesgue almost every } (x, y) \in \mathcal{X} \times \mathcal{Y}.$$

Thus, we have

$$\begin{aligned}
&\left\|\mathrm{RA}(x, (y_1, \ldots, y_n)) - R(x, \mathrm{Select}(x, (y_1, \ldots, y_n)))\right\|_\infty \\
&= \left\|\sum_{i=1}^{n} \alpha_i(x; \boldsymbol{y})\, r(x, y_i) - R(x, y_{i^*})\right\|_\infty \\
&\leq \sum_{i=1}^{n} \left\|\alpha_i(x; \boldsymbol{y})\, r(x, y_i) - R(x, y_{i^*})\right\|_\infty \\
&\leq \alpha_{i^*}(x, \boldsymbol{y}) \left\|r(x, y_{i^*}) - R(x, y_{i^*})\right\|_\infty + \sum_{j \neq i^*} \alpha_i(x; \boldsymbol{y}) \left\|r(x, y_i) - R(x, y_{i^*})\right\|_\infty \\
&\leq (1 - \varepsilon_1)\varepsilon_2 + \varepsilon_1 \max_{x, y, y^*} \left\|r(x, y) - R(x, y^*)\right\|_\infty .
\end{aligned}$$

Note that $\max_{x,y,y^*} \left\|r(x, y) - R(x, y^*)\right\|_\infty$ is finite since $\mathcal{X}, \mathcal{Y}$ are compact and r, R are continuous. Letting $\varepsilon_1, \varepsilon_2$ be small enough completes the proof. □

To summarize the analysis in this section, we showed that relational attention can approximate any computation composed of first selecting an object from a collection then computing a relation with that object. We can approximate any well-behaved selection criterion by formulating it in terms of an abstract preference preorder, and approximating the corresponding utility function (given by a Debreu representation theorem) by inner products of query and key feature maps. We can then approximate the target relation function similarly by inner products of a different set of query and key feature maps.

In the analysis above, we set aside the role of the symbols. Note that the function class this approximation result proves involves retrieving a relation from a selected object, but does not explicitly encode the identity of the selected object. Informally, the receiver knows that it has a particular relation with one of the objects in its context, and knows that this relation is with an object that was selected according to a particular selection criterion, but does not know the identity of the object beyond that. This is the purpose of adding symbols to relational attention—the retrieved relation is tagged with a symbol identifying the sender.

B ARCHITECTURE & IMPLEMENTATION DETAILS

In this section, we briefly discuss some details of implementation that may be of interest to some readers. Our code is publicly available through the project git repository and includes detailed instructions for reproducing our experimental results. We also provide links to experimental logs. Our code uses the PyTorch framework.

B.1 RELATIONAL ATTENTION AND DUAL-HEAD ATTENTION

The relational attention operation is defined as part of dual-head attention in Algorithm 1. We briefly mention some details of the implementation.

Learnable parameters. Let $n_h := n_h^{sa} + n_h^{ra}$ be the total number of sensory and relational heads. The learnable parameters are

- **Sensory attention heads.** For each head $h \in [n_h^{sa}]$:
  - Attention query/key projections: $W_{q,h}^{\mathrm{attn}}, W_{k,h}^{\mathrm{attn}} \in \mathbb{R}^{d_{\mathrm{model}} \times d_{\mathrm{key}}}$,
  - Value projections: $W_v^h \in \mathbb{R}^{d_{\mathrm{model}} \times d_h}$,
  - Output projection: $W_o^{sa} \in \mathbb{R}^{d_{\mathrm{model}} \times d_{\mathrm{model}}}$.
- **Relational attention heads.** For each head $h \in [n_h^{ra}]$ and each relation $\ell \in [d_r]$:
  - Attention query/key projections: $W_{q,h}^{\mathrm{attn}}, W_{k,h}^{\mathrm{attn}} \in \mathbb{R}^{d_{\mathrm{model}} \times d_{\mathrm{key}}}$,
  - Relation query/key projections: $W_{q,\ell}^{\mathrm{rel}}, W_{k,\ell}^{\mathrm{rel}} \in \mathbb{R}^{d_{\mathrm{model}} \times d_{\mathrm{proj}}}$,
  - Symbol projection: $W_s^h \in \mathbb{R}^{d_{\mathrm{model}} \times d_h}$,
  - Relation projection: $W_r^h \in \mathbb{R}^{d_r \times d_h}$,
  - Output projection: $W_o^{ra} \in \mathbb{R}^{d_{\mathrm{model}} \times d_{\mathrm{model}}}$.

We let $d_{\mathrm{key}}, d_h = d_{\mathrm{model}}/n_h$ to maintain the same dimension for the input and output objects. Similarly, we let $d_{\mathrm{proj}} = d_h \cdot n_h^{ra}/d_r$ so that the number of parameters is fixed as d_r varies. That is, we scale d_{proj} down as d_r increases; d_{proj} has the interpretation of being the dimensionality of the subspace on which we are computing comparisons. So, having a larger number of relations corresponds to a more fine-grained comparison between the two objects.

To model symmetric relations, we let $W_{q,\ell}^{\mathrm{rel}} = W_{k,\ell}^{\mathrm{rel}}$. Recall that this has the interpretation of computing a comparison between the same attributes in the pair of objects.

Note that the same d_r-dimensional relation is used for all n_h^{ra} attention heads, with a different learned linear map W_r^h for each head extracting the relevant aspects of the relation for that attention head and controlling the placement in the residual stream. This allows for useful computations to be shared across all heads. Note also that the head dimension $d_h = d_{\mathrm{model}}/n_h$ is defined in terms of the total number of attention heads and is the same for both sensory attention and relational attention. The output of each head is a d_h-dimensional vector. This means that after concatenating all the heads, the proportion in the final d_{model}-dimensional output that corresponds to each attention head type is proportional to the number of heads of that type. For example, if $n_h^{sa} = 6, n_h^{ra} = 2$, then 75% of the d_{model}-dimensional output is composed of the output of sensory attention heads and 25% is composed of the output of relational attention heads. This enables tuning the relative importance of each head type for the task.

Code. We briefly discuss the code implementing relational attention. We use `einsum` operations heavily in our implementation due to the flexibility they offer for implementing general tensor contractions. From Algorithm 1, recall that relational attention takes the form:

$$a_i^{(h)} \leftarrow \sum_j \alpha_{ij}^{(h)} \big(\boldsymbol{r}_{ij} W_r^h + s_j W_s^h \big), \tag{10}$$

where $\alpha_{ij}^{(h)}$ are the softmax attention scores for head $h \in [n_h^{ra}]$, $\boldsymbol{r}_{ij} \in \mathbb{R}^{d_r}$ are relation vectors, $s_j \in \mathbb{R}^{d_{\mathrm{model}}}$ is the symbol associated with the j-th input, and W_r^h, W_s^h map $\boldsymbol{r}_{ij}$ and s_j, respectively, to d_h-dimensional vectors. We assume those are already computed and focus on a particular portion of the computation of relational attention. We break up the computation as follows:

$$\sum_j \alpha_{ij}^{(h)} \big(\boldsymbol{r}_{ij} W_r^h + s_j W_s^h \big) = \sum_j \big(\alpha_{ij}^{(h)} s_j W_s^h \big) + \big(\sum_j \alpha_{ij}^{(h)} \boldsymbol{r}_{ij} \big) W_r^h. \tag{11}$$

Note that we factor out the W_r^h linear map and apply it after computing $\sum_j \alpha_{ij}^{(h)} \boldsymbol{r}_{ij}$. This is intentional, as will be explained below.

This can be computed in PyTorch via `einsum` operations as follows.

```
# sv: (b, n, n_h, d_h)
# attn_scores: (b, n_h, n, n)
# relations: (b, n, n, d_r)
# self.wr: (n_h, d_h, d_r)

attended_symbols = torch.einsum('bhij,bjhd->bihd', attn_scores, sv)
# shape: (b, n, n_h, d_h)

attended_relations = torch.einsum('bhij,bijr->bihr', attn_scores,
                                  relations)
# shape: (b, n, n_h, d_r)

attended_relations = torch.einsum('bihr,hdr->bihd', attended_relations,
                                  self.wr)
# shape: (b, n, n_h, d_h)

output = attended_symbols + attended_relations
# shape: (b, n, n_h, d_h)
```

Here, we assume `sv`, `attn_scores`, and `relations` are already computed, and focus on a particular part of the computation. `sv[:,:,h,:]` $= \boldsymbol{s}\, W_s^h$, corresponds to the symbols of each object in the context, `attn_scores[:,h,:,:]` $= \boldsymbol{\alpha}^h$ are the softmax attention scores, and `relations[:, i,j,:]` $= \boldsymbol{r}_{ij}$ are the relations, which can all be computed with simple matrix multiplication operations, very similar to the standard implementations of multi-head attention.

The first line corresponds to computing $\sum_j \alpha_{ij}^h s_j W_s^h$. The second line corresponds to computing $\sum_j \alpha_{ij}^h \boldsymbol{r}_{ij}$. The third line corresponds to applying the linear map W_r^h to the retrieved relations at each head. The reason we apply the map W_r^h after attending to the relations is for memory efficiency reasons. If we were to apply W_r^h first, we would need to manifest a tensor of dimension $b \times n \times n \times n_h^{ra} \times d_h$, which is of order $\mathcal{O}(b \cdot n^2 \cdot d_{\text{model}})$. Instead, by factoring out W_r^h and applying it after computing attention, we only need to manifest a tensor of dimension $b \times n \times n \times d_r$, which is much smaller since $d_r \ll d_{\text{model}}$. This tensor is contracted to a dimension $b \times n \times d_r$ first, *then* mapped up to $b \times n \times n_h^{ra} \times d_h$. This makes the memory footprint of relational attention of the same order as standard (sensory) attention when $d_r \asymp n_h$.

When using position-relative symbols, the implementation is adjusted since we need to compute

$$\sum_j \alpha_{ij}^{(h)} \left(\boldsymbol{r}_{ij} W_r^h + s_{j-i} W_s^h \right) \tag{12}$$

instead, where the symbol s_{j-i} sent now depends on both the sender j and the receiver i. Thus, we now compute a symbols tensor which is indexed by both the sender j and receiver i: `sv[i,j,h,:]` $= s_{j-i} W_s^h$. Then, the implementation is adjusted by replacing the first line in the code above with

```
    attended_symbols = torch.einsum('bhij,ijhd->bihd', attn_scores, sv)
```

The full implementation is made available through the project's github repository.

Composing relational attention to learn hierarchical relations. We remark that composing relational attention modules can be interpreted as representing hierarchical or higher-order relations. That is, relations between relations. An example of this is the relation tested in the `match pattern` task in the relational games benchmark. After one iteration of relational attention, an object's representation is updated with the relations it has with its context. A second iteration of relational attention now computes a representation of the relation between an object's relations and the relations of the objects in its context.

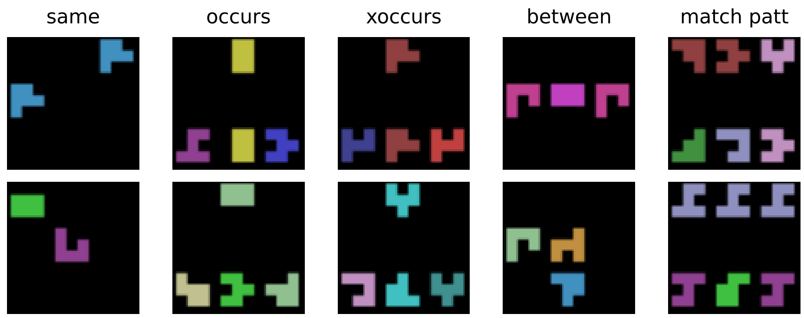

Figure 6: Examples of different tasks in the Relational Games benchmark. Each column corresponds to a different task in the benchmark. The top row is an example of a positive instance and the bottom row is an example of a negative instance.

B.2 Encoder and Decoder Blocks

We briefly mention a few configurations in our implementation that appear in our experiments. We aimed to make our implementation configurable to allow for various tweaks and optimizations that have been found in the literature for training Transformer models.

Symbol assignment. A shared symbol assignment module is used for all layers in the model. We explore three types of symbol assignment mechanisms: positional symbols, position-relative symbols, and symbolic attention. Different symbol assignment mechanisms are more well-suited to different tasks. We discuss ablation experiments we carried out on the effect of the symbol assignment mechanism in Appendix C.

MLP block. The MLP block uses a 2-layer feedforward network with a configurable activation function. The intermediate layer size is $d_{\mathrm{ff}} = 4 \cdot d_{\mathrm{model}}$ by default. We also use the SwiGLU "activation function" [46] in some of our experiments. SwiGLU is not merely an activation function, but is rather a neural network layer defined as the component-wise product of two linear transformations of the input. It is a type of gated linear unit [47] with the sigmoid activation replaced with a Swish activation [48], $\mathrm{SwiGLU}(x) = \mathrm{Swish}(xW + b) \otimes (xV + c)$. This is used in the Llama series of models and was found to be a useful modification [49].

Normalization. Either LayerNorm [50] or RMSNorm [51] can be used. Normalization can be performed post-attention, like in the original Transformer paper [4], or pre-attention as in [52].

Positional encoding. Our experiments use either learned positional embeddings or RoPE [29].

C Experimental Details & Further Discussion

C.1 Relational Games (Section 4.1)

Experimental details

Dataset details. The Relational Games benchmark datasets consists of $36 \times 36 \times 3$ RGB images depicting a 3×3 grid of objects which satisfy a particular visual relationship. The task is to identify whether a given relationship holds or not. The set of objects consists of simple geometric shapes. Examples of each task are presented in Figure 6. For example, in the `occurs` task, one object is present in the top row and three in the bottom row, and the task is to determine whether the object in the top row occurs (i.e., is among) the objects in the bottom row. The most difficult task in the benchmark is the `match pattern` task, where the grid contains a triplet of objects in the top row and another triplet of objects in the bottom row. Each triplet satisfies some relationship (e.g., ABC, ABA, ABB, or AAB), and the task is to determine whether the relation in the first triplet is the same as the relation in the second triplet. The difficulty in solving this task is that it requires parsing a second-order relation (a relation between relations). We remark that composing relational attention modules naturally captures this kind of hierarchical relations: the first relational attention operation produces objects representing relational information and the second would compute relations between those relations (i.e., second-order relations).

Model architectures. We use a Vision-Transformer-type architecture where the input image is split up into patches, flattened, and passed through the sequence model with added learned positional embeddings. We use average pooling at the end and pass through an MLP to produce the final prediction. We use a patch size of 12×12 which separates objects according to the grid structure. We note that in more general visual relational reasoning tasks where there isn't this type of grid structure, it would be appropriate to combine our approach with an object-discovery module such as Slot Attention [53].

We use 2-layer models. The *DAT* models use $d_{\text{model}} = 128$, $d_{\text{ff}} = 256$. One set of Transformer baselines uses the same, while another is larger with $d_{\text{model}} = 144$, $d_{\text{ff}} = 288$. All models use SwiGLU "activation", dropout rate = 0.1, and pre-LayerNormalization. For the *DAT* models, we use positional symbols as the symbol assignment mechanism. The composition of sensory and relational attention heads are depicted in the figure. In Figure 2, we use symmetric relations (i.e., imposing that $W_q^{\text{rel}} = W_k^{\text{rel}}$). Below, we also explore the effect of this inductive bias, evaluating variants without the symmetry constraint.

Training details. For each task and model, we evaluated learning curves by varying the training set size and training the model until convergence, then evaluating on a hold-out test set. For four out of five of the tasks, we evaluate learning curves within the range of 250 to $2,500$ samples, in increments of 250. For the more difficult `match pattern`, the range is from $5,000$ to $25,000$ in increments of $5,000$. The ranges were chosen based on the difficulty of the different tasks in order to identify the right "resolution". When evaluating learning curves, each training set is sampled randomly from the full dataset. For each task, model, and training set size, we repeat the experiment 5 times with different random seeds to compute approximate confidence intervals (accounting for randomness in sampling the dataset and random initialization). We use an Adam optimizer with a learning rate of 0.001, $\beta_1 = 0.9$, $\beta_2 = 0.99$, and a batch size of 512. We train for 50 epochs.

Further Discussion, Exploration, & Ablations

Comparison to previous relational architectures. Previous research has explored relational learning in synthetic settings, proposing various architectures with relational inductive biases. Here, we compare *DAT* to three such architectures: PrediNet [17], CoRelNet [20], and Abstractor [21]. Unlike *DAT*, these architectures use subtractive rather than additive relational inductive biases, imposing constraints on the types of learnable representations to improve relational learning efficiency. As a result, they are not general-purpose architectures and cannot be applied to broader domains such as language modeling. Nonetheless, it is useful to compare *DAT* against those architectures to explore the trade-offs of strong inductive biases and evaluate *DAT* in comparison to alternative approaches to relational learning. Figure 7 shows learning curves comparing *DAT* against those baselines. *DAT* performs competitively with previous relational architectures, generally outperforming PrediNet and Abstractor, while performing marginally worse than CoRelNet. It is relevant to note that CoRelNet incorporates strong task-specific inductive biases, and was partially designed with this benchmark in mind.

Ablation over symmetry. We performed an ablation over the *symmetry* inductive bias in the relations computed in relational attention. Our implementation exposes an argument which controls whether the relation $r(x, y) = (\langle W_{q,\ell}^{\text{rel}}, W_{k,\ell}^{\text{rel}} \rangle)_{\ell \in [d_r]} \in \mathbb{R}^{d_r}$ modeled in relational attention is constrained to be symmetric by setting $W_{q,\ell}^{\text{rel}} = W_{k,\ell}^{\text{rel}}$. Indeed, we find symmetry to be a useful inductive bias in this task. Figure 8 depicts learning curves for the two configurations of *DAT* comparing symmetric RA against asymmetric RA. We find that symmetry results in faster learning curves for both configurations.

C.2 Mathematical Problem-Solving (Section 4.2)

Experimental details

Dataset details. Saxton et al. [30] propose a benchmark to assess neural models' ability to perform mathematical reasoning. The dataset consists of a suite of tasks in free-form textual input/output format. The tasks cover several topics in mathematics, including arithmetic, algebra, and calculus. For each task, the authors programmatically generate 2×10^6 training examples and 10^4 validation examples. Questions have a maximum length of 160 characters and answers have a maximum length of 30 characters.

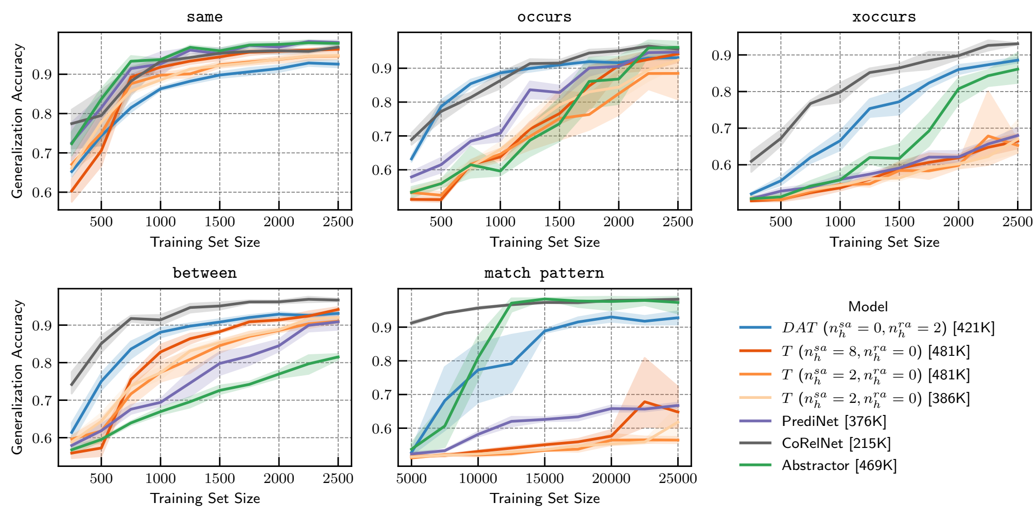

Figure 7: Learning curves on the Relational Games benchmark, comparing *DAT* against previously-proposed relational architectures. *DAT* performs competitively with previous relational architectures.

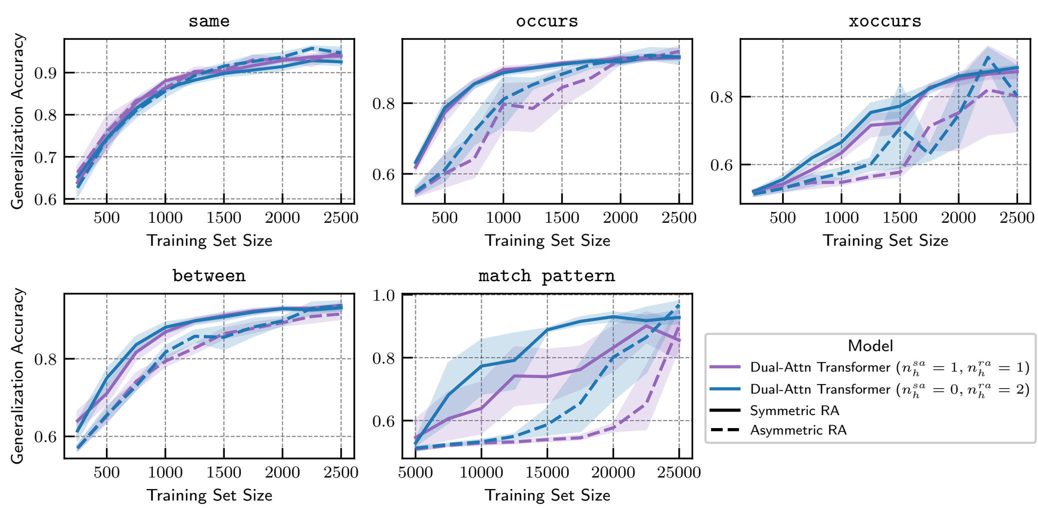

Figure 8: An ablation of the effect of symmetry in relational attention in the relational games experiments.

Model architectures. We use an encoder-decoder architecture for this experiment, treating it as a sequence-to-sequence task. We use character-level encoding with a common alphabet of size 85 containing small and upper case letters, digits 0-9, and symbols (e.g., `*, /, +, -`). We vary the number of layers to explore how performance scales with model size in *DAT* compared to standard Transformers. Each encode/decoder block uses ReLU activation, dropout rate = 0.1, and post-normalization. We use $d_{\text{model}} = 128, d_{\text{ff}} = 256$ for the *DAT* models and $d_{\text{model}} = 144, d_{\text{ff}} = 288$ in the Transformer models to control for parameter count and give the Transformer an advantage in the evaluation. Sinusoidal positional embeddings are used as the positional encoding method. For all models, the total number of attention heads (across self-attention and relational attention) is 8. For the Transformer model, there are only self-attention heads: $n_h^{sa} = 8$ for both the encoder and decoder. For *DAT*, we evaluated two configurations for the composition of head types, one with $n_h^{sa} = n_h^{ra} = 4$ in the encoder and $n_h^{sa} = 8, n_h^{ra} = 0$ in the decoder (i.e., standard Transformer Decoder), and one with $n_h^{sa} = 4 = n_h^{ra} = 4$ in the encoder and $n_h^{sa} = 4 = n_h^{ra} = 4$ in the decoder. The number of cross-attention heads in the decoder is 8 in all cases. No symmetry constraint is made

Task	Model	Parameter Count	# Layers	d_{model}	Encoder n_h^{sa}	Encoder n_h^{ra}	Decoder n_h^{sa}	Decoder n_h^{ra}	Accuracy
algebra__linear_1	Transformer	692K	2	128	8	0	8	0	$62.5 \pm 1.1\%$
	DAT	783K	2	128	4	4	8	0	$66.5 \pm 1.0\%$
	Transformer	871K	2	144	8	0	8	0	$64.0 \pm 1.5\%$
	DAT	1.09M	3	128	4	4	8	0	$68.1 \pm 6.5\%$
	Transformer	1.3M	3	144	8	0	8	0	$57.0 \pm 2.3\%$
	DAT	1.43M	4	128	4	4	8	0	$73.1 \pm 1.1\%$
	Transformer	1.7M	4	144	8	0	8	0	$53.2 \pm 1.1\%$
algebra__sequence_next_term	Transformer	692K	2	128	8	0	8	0	$91.1 \pm 0.2\%$
	DAT	783K	2	128	4	4	8	0	$91.6 \pm 0.6\%$
	Transformer	871K	2	144	8	0	8	0	$91.4 \pm 0.2\%$
	DAT	1.09M	3	128	4	4	8	0	$97.0 \pm 0.5\%$
	Transformer	1.3M	3	144	8	0	8	0	$96.1 \pm 0.5\%$
	DAT	1.43M	4	128	4	4	8	0	–
	Transformer	1.7M	4	144	8	0	8	0	$93.4 \pm 2.0\%$
calculus__differentiate	Transformer	692K	2	128	8	0	8	0	$99.9 \pm 0.0\%$
	DAT	783K	2	128	4	4	8	0	$100.0 \pm 0.0\%$
	Transformer	871K	2	144	8	0	8	0	$99.9 \pm 0.0\%$
	DAT	1.09M	3	128	4	4	8	0	–
	Transformer	1.3M	3	144	8	0	8	0	$99.9 \pm 0.0\%$
	DAT	1.43M	4	128	4	4	8	0	$100.0 \pm 0.0\%$
	Transformer	1.7M	4	144	8	0	8	0	$99.9 \pm 0.0\%$
polynomials__add	Transformer	692K	2	128	8	0	8	0	$83.3 \pm 0.1\%$
	DAT	783K	2	128	4	4	8	0	$85.6 \pm 0.0\%$
	Transformer	871K	2	144	8	0	8	0	$84.5 \pm 0.3\%$
	DAT	1.09M	3	128	4	4	8	0	$87.8 \pm 0.1\%$
	Transformer	1.3M	3	144	8	0	8	0	$86.4 \pm 0.3\%$
	DAT	1.43M	4	128	4	4	8	0	$88.7 \pm 0.0\%$
	Transformer	1.7M	4	144	8	0	8	0	$87.6 \pm 0.2\%$
polynomials__expand	Transformer	692K	2	128	8	0	8	0	$74.0 \pm 0.7\%$
	DAT	783K	2	128	4	4	8	0	$77.8 \pm 0.1\%$
	Transformer	871K	2	144	8	0	8	0	$74.1 \pm 0.6\%$
	DAT	1.09M	3	128	4	4	8	0	–
	Transformer	1.3M	3	144	8	0	8	0	$81.0 \pm 1.2\%$
	DAT	1.43M	4	128	4	4	8	0	$91.4 \pm 0.9\%$
	Transformer	1.7M	4	144	8	0	8	0	$89.2 \pm 0.5\%$

Table 2: Full results of mathematical problem-solving experiments. For each task, this table shows the mean test character-level accuracy $\pm$ the standard error of mean for each model configuration.

on relational attention. Position-relative symbols are used as the symbol assignment mechanism, and the symbol library is shared across all layers in both the encoder and decoder.

Training Details. Each model is trained on each task for 50 epochs. We use the Adam optimizer with $\beta_1 = 0.9, \beta_2 = 0.995$, a learning rate of 6×10^{-4}, and a batch size of 128. We evaluate and track the per-character accuracy over the course of training. We repeat this process 5 times for each combination of model and task with different random seeds to compute approximate confidence intervals.

Further Discussion, Exploration, & Ablations

Table 2 reports the full set of results obtained for this experiment, including certain configurations omitted from the figure in the main text.

C.3 Visual Processing (Section 4.3)

Experimental details

Dataset details. In this set of experiments, we use the CIFAR-10 and CIFAR-100 datasets [31] which are datasets of labeled small images. The CIFAR-10 dataset consists of $60,000$ 32×32 RGB images, evenly split across 10 classes. The CIFAR-100 dataset consists of $60,000$ RGB images of the same size, evenly split across 100 classes.

Model architectures. We use a *ViT*-style architecture [10]. RGB images are divided into 4×4 patches, flattened, linearly embedded into a vector, and fed through an Encoder. We use average pooling followed by an MLP to produce the final prediction. We evaluate 8-layer models with $d_{\text{model}} = d_{\text{ff}} = 384$, GeLU activation, Pre-LayerNormalization, and no dropout. The *ViT* model has $n_h^{sa} = 12$ standard self-attention heads, while the *DAT* model uses both sensory and relational heads, with an even split $n_h^{sa} = n_h^{ra} = 6$. In the main text, we use symmetric relations $\boldsymbol{r}_{ij}$ with the intuition that visual processing involves symmetric attribute-similarity relations. We also carried out experiments with asymmetric relations and discuss the results below. In *DAT*, we use position-relative symbols as the symbol assignment mechanism. Further, we use Grouped Query Attention [54] in *DAT* to reduce the parameter count to account for the added parameters in relational attention.

Training Details. We train for 100 epochs. We use the Adam optimizer with a learning rate schedule consisting of a gradual warmup to 10^{-3} in the first 5 epochs, followed by a cosine rate decay down to 10^{-5}. We use the hyperparameters $\beta_1 = 0.9, \beta_2 = 0.999$, and weight decay of $5 \cdot 10^{-5}$. We

Dataset	Model	Parameter Count	# Layers	d_{model}	n_h^{sa}	n_h^{ra}	Symmetric $\boldsymbol{r}_{ij}$	Accuracy
CIFAR-10	*ViT*	7.1M	8	384	12	0	NA	$86.4 \pm 0.1\%$
	ViDAT	6.0M	8	384	6	6	Yes	$89.7 \pm 0.1\%$
		6.6M	8	384	6	6	No	$89.5 \pm 0.1\%$
CIFAR-100	*ViT*	7.2M	8	384	12	0	NA	$68.8 \pm 0.2\%$
	ViDAT	6.1M	8	384	6	6	Yes	$70.5 \pm 0.1\%$
		6.7M	8	384	6	6	No	$70.5 \pm 0.1\%$

Table 3: Ablation over symmetry of $\boldsymbol{r}_{ij}$ in relational attention for image recognition experiments.

Dataset	Model	Parameter Count	# Layers	d_{model}	n_h^{sa}	n_h^{ra}	Accuracy
CIFAR-10	*ViT*	7.1M	8	384	12	0	$89.5 \pm 0.1\%$
	ViDAT	6.0M	8	384	6	6	$\mathbf{91.7 \pm 0.1\%}$
CIFAR-100	*ViT*	7.2M	8	384	12	0	$68.2 \pm 0.1\%$
	ViDAT	6.1M	8	384	6	6	$\mathbf{70.9 \pm 0.1\%}$

Table 4: Classification accuracy on CIFAR-10 and CIFAR-100 with AutoAugment data augmentation during training. Each training configuration is repeated 10 times with different random seeds; we report the mean accuracy $\pm$ the standard error of mean. *DAT* continues to outperform the standard Vision Transformer.

normalize the images channel-wise such that pixels have mean zero and unit standard deviation. In the results reported in Table 1 in the main text, we use random cropping, MixUp [32], and CutMix [33] as data augmentation techniques during training. We also report results using AutoAugment [55] below.

Further Discussion, Exploration, & Ablations

Effect of symmetry in $\boldsymbol{r}_{ij}$. In the main text, Table 1 reports *DAT* results with symmetric relations $\boldsymbol{r}_{ij}$ by imposing $W_q^{\text{rel}} = W_k^{\text{rel}}$. Here, we explore the effect of this choice. Table 3 compares *DAT* models with and without the symmetry constraint. We find no significant difference in performance. Though, we note the smaller parameter count in the symmetric variant.

Alternative data augmentation. In the main text, we use random cropping, MixUp, and CutMix data augmentation during training. Here, we report results on an alternative data augmentation technique: AutoAugment [55]. AutoAugment is an optimized set of data augmentation policies, found through a data-dependent automatic search procedure. At each mini-batch, a random sub-policy is chosen which consists of image processing operations such as translation, rotation, or shearing. Table 4 reports results using this data augmentation procedure. We continue to find that *ViDAT* outperforms the standard *ViT* model.

C.4 Language Modeling (Section 4.4)

Experimental details

Dataset details. The FineWeb-Edu [37] dataset is a curated dataset of text data. It is generated by filtering the large-scale FineWeb dataset for LLM pre-training [56] using an educational quality classifier trained on annotations generated by LLama3-70B-instruct. FineWeb-Edu has been shown to outperform FineWeb on several benchmarks, demonstrating the importance of data *quality*. We train our language models on a random subset of 10 billion tokens of FineWeb-Edu.

Model Architectures. We use a Decoder-only architecture, with causal attention for autoregressive language modeling. We vary model size to explore the scaling properties of *DAT* with respect to both model size and data size, comparing to the scaling properties of standard Transformers. Our architectural hyperparameters follow common choices at different model scales, based on scaling analyses performed for Transformers [56]. We explore 3 model scales: 350M ($d_{\text{model}} = 1024, n_h = 16, L = 24$), 750M ($d_{\text{model}} = 1536, n_h = 24, L = 24$), and 1.3B ($d_{\text{model}} = 2048, n_h = 32, L = 24$) parameters. We use $d_{\text{ff}} = 4 \cdot d_{\text{model}}$, GeLU activation, RoPE positional encoding, no bias, no dropout, and Pre-LayerNormalization. We use the GPT2 tokenizer [7]. We use symbolic attention as the symbol assignment mechanism, with the number of symbols in the symbol library scaling with model size: 1024 symbols and 8 heads for the 350M and 750M scale models, and 2048 symbols with 16 heads for the 1.3B scale model. We also increase the relation dimension with model size. We don't impose a symmetry constraint, with the intuition that linguistic relations can be asymmetric. We use Grouped Query Attention in the *DAT* models to reduce parameter count to account for the added parameters in relational attention, making them smaller overall compared to the Transformer baselines at each parameter scale.

Training Details. We train for 10B Tokens, with each batch containing $524,288$ tokens, split into context windows of $1,024$ tokens. We use gradient accumulation to fit micro-batches into memory. We use the AdamW optimizer with a maximum learning rate of 6×10^{-4} and minimum learning rate of 6×10^{-5}, first linearly warming up over the first 715 steps, then decaying back down with a cosine schedule. We use $\beta_1 = 0.9, \beta_2 = 0.95$ and a weight decay of 0.1. We also use gradient clipping to unit norm.

Further Discussion, Exploration, & Ablations

Figure 4 in the main text depicts the scaling properties of a *DAT* language model with respect to model size and data size compared to a standard Transformer. Here, we provide a few additional representations of the results. Table 5 reports the end-of-training validation perplexity of the different models.

Figure 9 depicts training curves for the different model scales. We observe a power law scaling of the validation loss with respect to number of training tokens. This matches the neural scaling laws [8], which suggest that validation loss ought to scale roughly as $d^{-\alpha}$ where d is the amount of training data and the exponent α is a constant that depends on model architecture, training details, etc.

Table 5: End-of-training validation perplexity in language modeling on FineWeb-Edu dataset.

Model	Param count	# Tokens	d_{model}	n_{layers}	n_h^{sa}	n_h^{ra}	d_r	n_{kv}^h	Perplexity ↓
Transformer	353M	10B	1024	24	16	-	-	-	16.94
DAT	343M	10B	1024	24	8	8	64	4	16.09
Transformer	757M	10B	1536	24	24	-	-	-	14.65
DAT	734M	10B	1536	24	12	12	64	6	14.31
Transformer	1.31B	10B	2048	24	32	-	-	-	13.63
DAT	1.27B	10B	2048	24	16	16	128	8	13.43

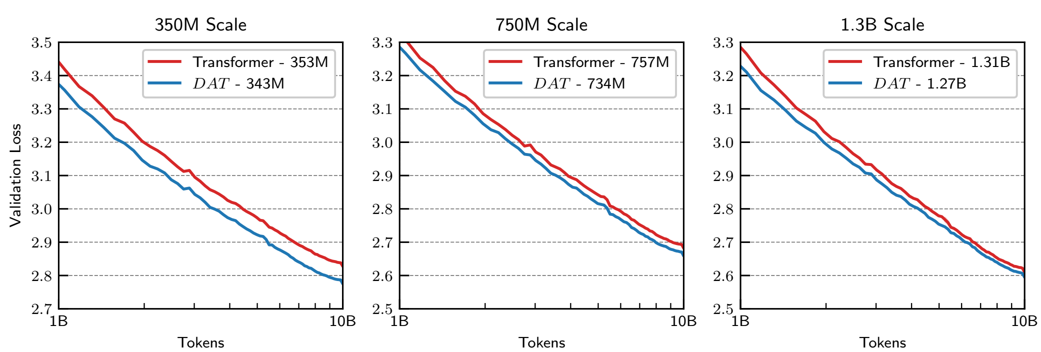

Figure 9: Validation loss on a logarithmic scale to examine data scaling laws. Dual Attention Transformer language models obey similar scaling laws as standard Transformers with respect to the amount of training data, while consistently achieving smaller loss at multiple model scales.

D COMPARISON TO ALTABAA ET AL. [21]: ABSTRACTORS AND RELATIONAL CROSS-ATTENTION

A closely related work is Altabaa et al. [21], which proposes a Transformer-based module called the "Abstractor" with relational inductive biases. The core operation in the Abstractor is a variant of attention dubbed "relational cross-attention" (RCA). In this section, we will discuss the relation between the Dual Attention Transformer and the Abstractor.

D.1 COMPARISON BETWEEN RA (THIS WORK) AND RCA [21]

Altabaa et al. [21] propose a variant of attention called relational cross-attention which shares some characteristics with our proposal of what we're calling "relational attention" in this work. In this discussion, we will use the acronyms RCA and RA, respectively to distinguish between the two.

RCA processes a sequence of objects $\boldsymbol{x} = (x_1, \dots, x_n)$ and produces a sequence of objects $\boldsymbol{x}' = (x_1', \dots, x_n')$ via the following operation

$$\begin{aligned} \boldsymbol{x}' &\leftarrow \sigma_{\text{rel}} \left(\phi_q(\boldsymbol{x}) \phi_k(\boldsymbol{x})^\intercal \right) \boldsymbol{s}, \\ \boldsymbol{s} &= \text{SymbolRetriever}(\boldsymbol{x}) \end{aligned}$$

where ϕ_q, ϕ_k are query and key transformations, and the symbols $\boldsymbol{s}$ take the same role as in this work. σ_{rel} is referred to as a "relation activation". It may be either softmax or an element-wise activation (e.g., tanh, sigmoid, or linear). For the purposes of this discussion, let us consider $\sigma_{\text{rel}} = \text{Softmax}$, which was used in the majority of the experiments in [21].

To facilitate the discussion, let us write RA and RCA side-by-side using a common notation.

RA (this work)

$$\begin{aligned} (x_1', \dots, x_n') &\leftarrow \text{RA}(\boldsymbol{x}; S_{\text{lib}}), \\ x_i' &= \sum_{j=1}^{n} \alpha_{ij} \left(r(x_i, x_j)\, W_r + s_j\, W_s \right), \\ \boldsymbol{\alpha} &= \text{Softmax}\left(\phi_q(\boldsymbol{x}) \phi_k(\boldsymbol{x})^\intercal \right), \\ r(x, y) &= \left(\left\langle \phi_{q,\ell}^{\text{rel}}(x), \phi_{k,\ell}^{\text{rel}}(y) \right\rangle \right)_{\ell \in [d_r]}, \\ (s_1, \dots, s_n) &= \text{SymbolRetriever}(\boldsymbol{x};\, S_{\text{lib}}) \end{aligned}$$

RCA [21]

$$\begin{aligned} (x_1', \dots, x_n') &\leftarrow \text{RCA}(\boldsymbol{x}; S_{\text{lib}}) \\ x_i' &= \sum_{j=1}^{n} \alpha_{ij}\, s_j, \\ \boldsymbol{\alpha} &= \text{Softmax}\left(\phi_q(\boldsymbol{x}) \phi_k(\boldsymbol{x})^\intercal \right), \\ (s_1, \dots, s_n) &= \text{SymbolRetriever}(\boldsymbol{x};\, S_{\text{lib}}) \end{aligned}$$

RCA can be understood as self-attention, but the values are replaced with symbols (i.e., $\text{Attention}(Q \leftarrow \boldsymbol{x},\, K \leftarrow \boldsymbol{x},\, V \leftarrow \boldsymbol{s})$). By viewing the attention scores α_{ij} as relations, this has the effect of producing a relation-centric representation. The rationale is that in standard self-attention, the attention scores form a type of relation, but these relations are only used as an intermediate processing step in an information-retrieval operation. The relations encoded in the attention scores are entangled with the object-level features, which have much greater variability. This thinking also motivates the design of RA in the present work.

RCA can be understood as computing a pairwise relation $\langle \phi_q^{\text{attn}}(x_i), \phi_k^{\text{attn}}(x_j) \rangle$ between x_i and each x_j in the context, and retrieving the symbol s_j associated with the object x_j with which the relation is strongest. That is, RCA treats the relations and the attention scores as the same thing. By contrast, the attention operation and computation of relations are separate in RA. The attention component is modeled by one set of query/key maps $\phi_q^{\text{attn}}, \phi_k^{\text{attn}}$ and the relation component is modeled by another set of query/key maps $(\phi_{q,\ell}^{\text{rel}}, \phi_{k,\ell}^{\text{rel}})_{\ell \in [d_r]}$.

The intuitive reason for this choice is that, for many tasks, the optimal "selection criterion" will be different from the task-relevant relation. For example, in a language modeling task, you may want to attend to objects on the basis of proximity and/or syntax while being interested in a relation based on semantics. Similarly, in a vision task, you may want to attend to objects on the basis of proximity, while computing a relation across a certain visual attribute. Thus, the relational attention mechanism proposed in this work offers greater flexibility and expressivity compared to RCA.

In RA, the symbols maintain the role of identifying the sender. But instead of being the whole message, they are attached to a relation.

D.2 Comparison between *DAT* and the Abstractor

We now briefly discuss the differences in the corresponding model architectures. Altabaa et al. [21] propose an encoder-like module called the Abstractor which consists of essentially replacing self-attention in an Encoder with relational cross-attention. That is, it consists of iteratively performing RCA followed by an MLP. The paper proposes several ways to incorporate this into the broader Transformer architecture. For example, some of the experiments use a `Encoder` → `Abstractor` → `Decoder` architecture to perform a sequence-to-sequence task. Here, the output of a standard Transformer Encoder is fed into an Abstractor, and the Decoder cross-attends to the output of the Abstractor. In another sequence-to-sequence experiment, Altabaa et al. [21] use an architecture where the Decoder cross-attends to both the Encoder and the Abstractor, making use of both sensory and relational information. In particular, the standard encoder and decoder blocks are the same (focusing on sensory information), but an additional module is inserted in between with a relational inductive bias.

By contrast, our approach in this paper is to propose novel encoder and decoder architectures imbued with two distinct types of attention heads, one with an inductive bias for sensory information and the other with an inductive bias for relational information. This has several potential advantages. The first is versatility and generality. The Abstractor architectures that were explored in [21] only explicitly support sequence-to-sequence or discriminative tasks. For example, they do not support autoregressive models like modern decoder-only language models (e.g., of the form we experiment with in Section 4.4). Moreover, even in sequence-to-sequence tasks, Abstractor architectures only support relational processing over the input sequence, but they do not support relational processing over the target sequence (since the decoder does not have RCA). Another potential advantage of *DAT* is simplicity. The Abstractor paper proposes several architectures and configurations for the Encoder/Abstractor/Decoder modules, introducing several hyperparameters that are not trivial to choose. Moreover, it is unclear how to interpret this kind of architecture as the number of layers increases, and the original paper does not experiment with scaling up the number of layers. The final potential advantage is increased expressivity. In *DAT*, the two types of attention heads exist side by side in each layer. This allows relational attention heads to attend to the output of the self-attention heads at the previous layer, and vice-versa. This yields broader representational capacity, and potentially more interesting behavior as we scale the number of layers.

D.3 How would RCA perform in an *DAT*-style dual head-type architecture?

One question one might ask is: how would an *DAT*-style dual head-type architecture perform if we used Altabaa et al. [21]'s RCA instead of the RA head-type proposed in this work? We carried out a few ablation experiments to answer this question.

Figure 10 compares learning curves on the relational games benchmark between standard *DAT* (with RA-heads) and a version of *DAT* with Altabaa et al. [21]'s RCA heads. We find that the two models perform similarly, with most differences small enough to be within the margin of error. This figure depicts the configuration with asymmetric RA and positional symbols.

Figure 11 depicts the validation loss curves on a small-scale language modeling experiment based on the Tiny Stories dataset [57], comparing standard *DAT* against a version with RCA heads. Here, we find that our relational attention heads yield better-performing models, with the RCA-head variant of *DAT* performing no better than a standard Transformer with a matching total number of heads.

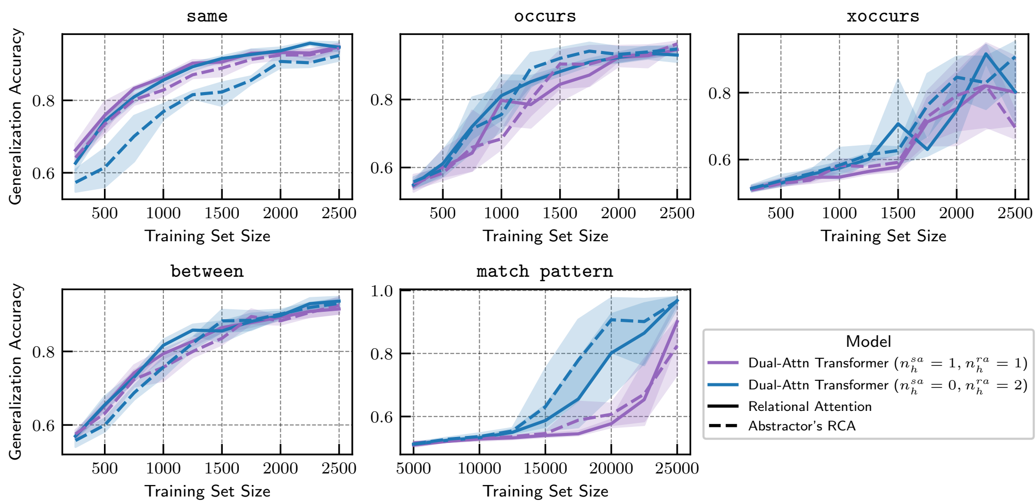

Figure 10: Learning curves for *DAT* with RA compared with *DAT* with RCA on the relational games benchmark. The performance is similar, with most differences within the margin of error.

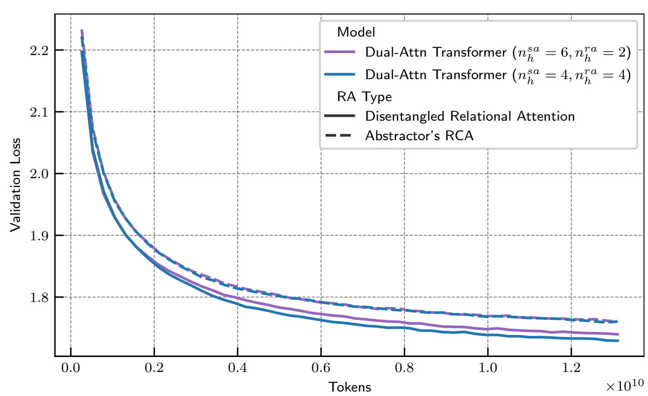

Figure 11: Ablation of relational attention type. The solid line depicts the form of relational attention proposed in this work. The dotted line depicts RCA as proposed by Altabaa et al. [21]. We find that our relational attention mechanism performs better, whereas RCA performs no better than a Transformer.